

# A view of mini-batch SGD via generating functions: conditions of convergence, phase transitions, benefit from negative momenta

Maksim Velikanov    Denis Kuznedelev    Dmitry Yarotsky  
{maksim.velikanov, denis.kuznedelev, d.yarotsky}@skoltech.ru  
Skolkovo Institute of Science and Technology

## Abstract

Mini-batch SGD with momentum is a fundamental algorithm for learning large predictive models. In this paper we develop a new analytic framework to analyze mini-batch SGD for linear models at different momenta and sizes of batches. Our key idea is to describe the loss value sequence in terms of its generating function, which can be written in a compact form assuming a diagonal approximation for the second moments of model weights. By analyzing this generating function, we deduce various conclusions on the convergence conditions, phase structure of the model, and optimal learning settings. As a few examples, we show that 1) the optimization trajectory can generally switch from the "signal-dominated" to the "noise-dominated" phase, at a time scale that can be predicted analytically; 2) in the "signal-dominated" (but not the "noise-dominated") phase it is favorable to choose a large effective learning rate, however its value must be limited for any finite batch size to avoid divergence; 3) optimal convergence rate can be achieved at a negative momentum. We verify our theoretical predictions by extensive experiments with MNIST and synthetic problems, and find a good quantitative agreement.

## 1 Introduction

The fundamental algorithm of learning large predictive models is the mini-batch Stochastic Gradient Descent (SGD) [38, 8] with momentum [35]:

$$\mathbf{w}_{t+1} = \mathbf{w}_t + \mathbf{v}_{t+1}, \quad \mathbf{v}_{t+1} = -\alpha_t \nabla_{\mathbf{w}} L_{B_t}(\mathbf{w}_t) + \beta_t \mathbf{v}_t. \quad (1)$$

Here,  $L_B(\mathbf{w}) = \frac{1}{b} \sum_{i=1}^b l(f(\mathbf{x}_i, \mathbf{w}), y_i)$  is the sampled loss of a model  $\hat{y} = f(\mathbf{x}, \mathbf{w})$ , computed using a pointwise loss  $l(\hat{y}, y)$  on a mini-batch  $B = \{(\mathbf{x}_i, y_i)\}_{i=1}^b$  of  $b$  data points representing the target function  $y = f^*(\mathbf{x})$ . The sampled loss  $L_B(\mathbf{w})$  is a noisy estimate of the true (expected) loss  $L(\mathbf{w}) = \mathbb{E}_{(\mathbf{x}, y)} l(f(\mathbf{x}, \mathbf{w}), y)$  recovered in the limit  $b \rightarrow \infty$ . This *sampling noise* is unavoidable when training large models, but decreases as the batch size is increased. We will assume that the stochasticity in the iterations (1) is only associated with this sampling noise (note that this assumption is very different from a popular assumption of *additive* noise which may be, e.g., due to numerical errors, see Section F).

The term  $\mathbf{v}_n$  represents the *momentum* which is widely used and well-known to significantly improve convergence both generally [36] and in the context of deep learning [44]. Typically,  $\beta_t$  are assigned values from  $[0, 1)$  close to 1, e.g. 0.9 or 0.99. For constant learning rates  $\alpha$  and momenta  $\beta$ , the ratio  $\alpha_{\text{eff}} = \alpha / (1 - \beta) = \alpha + \alpha\beta + \alpha\beta^2 + \dots$  is the *effective learning rate* reflecting the accumulated effect of multiple iterations [45, 50]. We will always assume that  $|\beta| < 1$ , but allow  $\beta$  to be negative.

The goal of the present work is to derive possibly explicit and easy-to-use analytic evolution laws for the SGD (1) applicable to modern overparameterized deep neural networks trained on real world

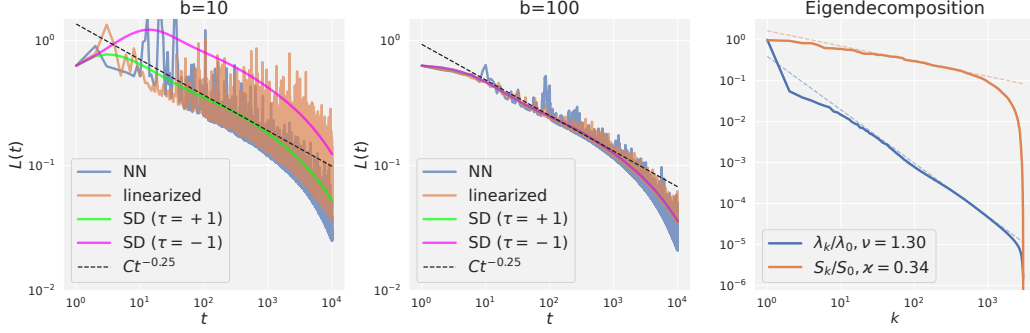


Figure 1: **Left, center:** Loss trajectories of different training regimes on MNIST for batch sizes 10 and 100. Actual nonlinear neural network (NN) is reasonably well approximated by the linearized model and its SD approximation with  $\tau = 1$  (see Section 2). **Right:** NTK eigenvalues  $\lambda_k$  and partial sums  $S_k = \sum_{l=k}^N c_l^2$  of squared coefficients  $c_k$  in the expansion of initial error vector over respective eigenvectors. Experimental curves are fitted to the asymptotic power laws  $L(t) \propto t^{-\xi}$ ,  $\lambda_k \propto k^{-\nu}$ ,  $S_k \propto k^{-\kappa}$  resulting in  $\nu \approx 1.30$ ,  $\kappa \approx 0.34$ ,  $\xi \approx 0.25 \approx \frac{\kappa}{\nu}$ .

datasets such as MNIST. We argue now which further assumptions would be reasonable for that. First, in many (though not all) cases the nonlinear network training is reasonably well approximated [29] by the linearized NTK regime [22], in which the loss  $L$  is quadratic with an explicit kernel matrix. Accordingly, from now on we restrict our attention to quadratic problems. Next, modern networks are usually overparameterized, and the respective problems are highly ill-conditioned. Moreover, one can often observe particular laws – typically, power laws – governing the distribution of eigenvalues and target coefficients (see [12, 2, 29, 10, 27, 14, 1, 7, 3, 6] and Figure 1). We expect taking these into account to lead to reasonably accurate evolution laws. In particular, this naturally requires us to adopt the abstraction of optimization in infinitely many dimensions.

We stress that our approach is different from the more common approach focused on general upper bounds for convergence rates. To illustrate this, recall the classical bounds for the basic (non-stochastic) gradient descent [36]. Assuming  $\inf_{\mathbf{w}} L(\mathbf{w}) = 0$ , the bound for the non-strongly-convex quadratic optimization reads  $L(\mathbf{w}_t) \leq \|\mathbf{w}_0 - \mathbf{w}_*\|^2 / (4\alpha\epsilon t) = O(1/t)$ , while in the strongly convex case  $L(\mathbf{w}_t) \leq (\lambda_{\max}/2) \|\mathbf{w}_0 - \mathbf{w}_*\|^2 (\frac{\lambda_{\max} - \lambda_{\min}}{\lambda_{\max} + \lambda_{\min}})^{2t} = O(q^t)$ ,  $q < 1$ . One might expect these formulas to reasonably describe the training loss trajectory of a MNIST classifier at large batch sizes. In reality, however, this trajectory looks rather differently – it rather falls off as  $\propto t^{-0.25}$  up to a large number of iterations ( $\sim 10^3 - 10^4$ , see Figure 1). This effect, along with the exponent 0.25, can be explained using the spectral power laws associated with this problem [33, 48].

The main contribution of our paper is a new analytic framework for the study of mini-batch SGD in the above setting. Its first step (Section 2) is a “spectral diagonal approximation” for the evolution of second moments of the loss spectral components. The next step (Section 3) is a description of this evolution in terms of generating functions. The remainder of the paper (Section 4) uses this framework to address various practically important questions:

1. **Convergence criteria.** We derive a precise condition of loss convergence in terms of the problem spectrum  $\lambda_k$  and show that for  $\beta$  close to 1 this condition simplifies to  $\alpha_{\text{eff}} \lesssim 2b/\lambda_{\text{crit}}$ , where  $\lambda_{\text{crit}}$  is the critical regularization value at which the effective dimension of the problem equals 1.
2. **Phase transitions.** For non-strongly convex problems we show that our model exhibits distinct “signal-dominated” and “noise-dominated” convergence regimes (previously known for SGD without momenta [47]) depending on the spectral tails of eigenvalues and target expansion coefficients. We derive exact loss asymptotics for these regimes. We show that the noise-dominated regime is typically preceded by a time interval of signal-dominated regime, with transition occurring on a time scale  $t_{\text{trans}}$  that we predict analytically. We also predict analytically the time scale  $t_{\text{blowup}}$  of loss divergence for divergent models.
3. **Hyperparameter and budget optimization.** We show that in the signal-dominated regime it is favorable to choose large effective learning rates  $\alpha_{\text{eff}}$ . However, because of the stability

constraint  $\alpha_{\text{eff}} \lesssim 2b/\lambda_{\text{crit}}$ , admissible  $\alpha_{\text{eff}}$  are limited if batch size  $b < \infty$  (in stark contrast to noiseless GD). In agreement with earlier works, we find that the loss obtained with an optimal choice of  $\alpha, \beta$  can be approximately expressed as a function of the total computation budget  $bt$ . In contrast to the signal-dominated phase, in the noise-dominated phase it is counter-productive to use large effective learning rates.

4. **Negative momenta.** It is common to use SGD with momentum  $\beta \in (0, 1)$ . We find that in the signal-dominated regime it is always advantageous to include in SGD a momentum  $\beta > 0$ , but in the noise-dominated regime it may actually be advantageous to choose  $\beta < 0$ .

For lack of space, related work is described in Appendix A and experimental details in Appendix E.

## 2 The setting and the *Spectral Diagonal* approximation

We consider a linear model  $f(\mathbf{x}, \mathbf{w}) = \langle \mathbf{w}, \psi(\mathbf{x}) \rangle$  with non-linear features  $\psi(\mathbf{x})$  trained to approximate a target function  $y^*(\mathbf{x})$  by minimizing quadratic loss  $L(\mathbf{w}) = \frac{1}{2N} \sum_{i=1}^N (\langle \mathbf{w}, \psi(\mathbf{x}_i) \rangle - y^*(\mathbf{x}_i))^2$  over training dataset  $\mathcal{D} = \{\mathbf{x}_i\}_{i=1}^N$ . The model's Hessian is given by  $\mathbf{H} = \frac{1}{N} \sum_{i=1}^N \psi(\mathbf{x}_i) \otimes \psi(\mathbf{x}_i)$  and the tangent kernel  $K(\mathbf{x}, \mathbf{x}') = \langle \psi(\mathbf{x}), \psi(\mathbf{x}') \rangle$ . Assuming that the target function is representable as  $y^*(\mathbf{x}) = \langle \mathbf{w}^*, \psi(\mathbf{x}) \rangle$ , the loss takes the form  $L(\mathbf{w}) = \frac{1}{2} \langle \mathbf{w} - \mathbf{w}^*, \mathbf{H}(\mathbf{w} - \mathbf{w}^*) \rangle$ . We allow model parameters to be either finite dimensional vectors or belong to a Hilbert space  $\mathcal{H}$ . Similarly, dataset  $\mathcal{D}$  can be either finite ( $N < \infty$ ) or infinite, and in the latter case we only demand finite norm of the target function  $y^*(\mathbf{x})$  but not of the solution  $\mathbf{w}^*$ . Note that this setting is quite rich and can accommodate general kernel methods, linearization of practical neural networks, and infinitely wide neural networks in the NTK regime (see Appendix B for details).

Denoting deviation from the optimum as  $\Delta \mathbf{w} \equiv \mathbf{w} - \mathbf{w}^*$ , we can write a single SGD step at iteration  $t$  with a randomly chosen batch  $B_t$  of size  $b$  as

$$\begin{pmatrix} \Delta \mathbf{w}_{t+1} \\ \mathbf{v}_{t+1} \end{pmatrix} = \begin{pmatrix} \mathbf{I} - \alpha_t \mathbf{H}(B_t) & \beta_t \mathbf{I} \\ -\alpha_t \mathbf{H}(B_t) & \beta_t \mathbf{I} \end{pmatrix} \begin{pmatrix} \Delta \mathbf{w}_t \\ \mathbf{v}_t \end{pmatrix}, \quad \mathbf{H}(B_t) \equiv \frac{1}{b} \sum_{i \in B_t} \psi(\mathbf{x}_i) \otimes \psi(\mathbf{x}_i). \quad (2)$$

An important feature of the multiplicative noise introduced by the random choice of  $B_t$  is that the  $n$ 'th moments of parameter and momentum vectors  $\Delta \mathbf{w}_{t+1}, \mathbf{v}_{t+1}$  in dynamics (2) are fully determined from the same moments at the previous step  $t$ . As our loss function is quadratic, we focus on the second moments

$$\mathbf{C} \equiv \mathbb{E}[\Delta \mathbf{w} \otimes \Delta \mathbf{w}], \quad \mathbf{J} \equiv \mathbb{E}[\Delta \mathbf{w} \otimes \mathbf{v}], \quad \mathbf{V} \equiv \mathbb{E}[\mathbf{v} \otimes \mathbf{v}], \quad \Sigma \equiv \begin{pmatrix} \mathbf{C} & \mathbf{J} \\ \mathbf{J}^\dagger & \mathbf{V} \end{pmatrix}. \quad (3)$$

Then the average loss is  $\mathbb{E}[L(\mathbf{w})] = \frac{1}{2} \text{Tr}(\mathbf{H}\mathbf{C})$  and for combined second moment matrix we have

**Proposition 1.** *Consider SGD (1) with learning rates  $\alpha_t$ , momentum  $\beta_t$ , batch size  $b$  and random uniform choice of the batch  $B_t$ . Then the update of second moments (3) is*

$$\begin{pmatrix} \mathbf{C}_{t+1} & \mathbf{J}_{t+1} \\ \mathbf{J}_{t+1}^\dagger & \mathbf{V}_{t+1} \end{pmatrix} = \begin{pmatrix} \mathbf{I} - \alpha_t \mathbf{H} & \beta_t \mathbf{I} \\ -\alpha_t \mathbf{H} & \beta_t \mathbf{I} \end{pmatrix} \begin{pmatrix} \mathbf{C}_t & \mathbf{J}_t \\ \mathbf{J}_t^\dagger & \mathbf{V}_t \end{pmatrix} \begin{pmatrix} \mathbf{I} - \alpha_t \mathbf{H} & \beta_t \mathbf{I} \\ -\alpha_t \mathbf{H} & \beta_t \mathbf{I} \end{pmatrix}^T + \gamma \alpha_t^2 \begin{pmatrix} \hat{\mathbf{D}}\mathbf{C}_t & \hat{\mathbf{D}}\mathbf{C}_t \\ \hat{\mathbf{D}}\mathbf{C}_t & \hat{\mathbf{D}}\mathbf{C}_t \end{pmatrix} \quad (4)$$

The second term represents sampling noise and is given by

$$\hat{\mathbf{D}}\mathbf{C} = \frac{1}{N} \sum_{i=1}^N \langle \psi(\mathbf{x}_i), \mathbf{C}\psi(\mathbf{x}_i) \rangle \psi(\mathbf{x}_i) \otimes \psi(\mathbf{x}_i) - \mathbf{H}\mathbf{C}\mathbf{H} \quad (5)$$

with the amplitude  $\gamma = \frac{N-b}{(N-1)b}$  simplifying to  $\gamma = \frac{1}{b}$  in the large dataset limit  $N \rightarrow \infty$ .

While dynamics (4) is already linear and deterministic, we proceed to further simplifications. Let  $\lambda_k, \mathbf{u}_k$  be the eigenvalues and eigenvectors of  $\mathbf{H}$  with eigenvalues sorted in the decreasing order, and for any matrix  $\mathbf{K}$  denote its  $kl$  matrix elements in the eigenbasis of  $\mathbf{H}$  by  $K_{kl} \equiv \langle \mathbf{u}_k, \mathbf{K}\mathbf{u}_l \rangle$ . In particular, we have  $L(\mathbf{w}) = \frac{1}{2} \sum_k C_{kk} \lambda_k$ . Note that in the absence of noise in (4) different  $kl$  elements  $C_{kl}$  evolve independently from each other and we can consider only the diagonal part  $k = l$  that we are interested in. To partially preserve this convenient structure in the presence of noise we

introduce a family of *Spectral Diagonal* (SD) approximations  $\hat{D} \approx \hat{D}_{SD}$  of the sampling noise term (5), indexed by parameter  $\tau$ :

$$(\hat{D}_{SD}(\tau)\mathbf{C})_{kk} = \lambda_k \sum_l \lambda_l C_{ll} - \tau \lambda_k^2 C_{kk}. \quad (6)$$

Note first that the SD approximation keeps the diagonal part  $k = l$  invariant under SGD dynamics (4), which allows us to completely ignore the  $k \neq l$  elements as long as we are only interested in the average loss. Second, interaction between different diagonal elements  $k$  happens only through scalar “mean field”  $\sum_l \lambda_l C_{ll} = 2\mathbb{E}[L(\mathbf{w})]$ .

It turns out that SD approximations naturally arise in a number of theoretical scenarios and also quite accurately describe experiments with both realistic and synthetic data:

1. We prove that the SD approximation with  $\tau = 1$  is exact for translation invariant problems (Proposition 2 below).
2. If features  $\psi(\mathbf{x})$  have Gaussian distribution w.r.t.  $\mathbf{x} \sim \mathcal{D}$ , the SD approximation with  $\tau = -1$  is exact:  $(\hat{D}\mathbf{C})_{kk} = (\hat{D}_{SD}(\tau = -1)\mathbf{C})_{kk}$  for any  $\mathbf{C}$  (see [7]).
3. In our experiments on MNIST, the loss trajectories are very well described by SD approximation with  $\tau = 1$  (see Figs. 1, 2 and Appendix E).

**Proposition 2.** *Consider a translation invariant problem with dataset forming a regular grid  $\mathcal{D} = \{\mathbf{x}_{\mathbf{i}} = (\frac{2\pi i_1}{N_1}, \dots, \frac{2\pi i_d}{N_d})\}$ ,  $\mathbf{i} \in (\mathbb{Z}/N_1\mathbb{Z}) \times \dots \times (\mathbb{Z}/N_d\mathbb{Z})$  on a  $d$ -dimensional torus  $\mathbb{S}^d$  and with translation invariant kernel  $K(\mathbf{x}, \mathbf{x}') = K(\mathbf{x} - \mathbf{x}')$ . Then  $(\hat{D}\mathbf{C})_{kk} = (\hat{D}_{SD}(\tau = 1)\mathbf{C})_{kk}$ .*

SD approximation with  $\tau = 1$  has a clear interpretation. Note that the loss at the  $i$ ’th data point  $\mathbf{x}_i$  can be written as  $L_i = \frac{1}{2} \langle \psi(\mathbf{x}_i), \mathbf{C}\psi(\mathbf{x}_i) \rangle$  and that the feature vector at  $\mathbf{x}_i$  is decomposed over the eigenvectors  $\mathbf{u}_k$  with squared coefficients  $\psi_{ki}^2 \equiv \langle \mathbf{u}_k, \psi(\mathbf{x}_i) \rangle^2 = \langle \mathbf{u}_k, \psi(\mathbf{x}_i) \otimes \psi(\mathbf{x}_i) \mathbf{u}_k \rangle$ . Then the equality  $(\hat{D}\mathbf{C})_{kk} \approx (\hat{D}_{SD}(\tau = 1)\mathbf{C})_{kk}$  takes the form

$$\frac{1}{N} \sum_{i=1}^N 2L_i \psi_{ki}^2 \approx \left( \frac{1}{N} \sum_{i=1}^N 2L_i \right) \left( \frac{1}{N} \sum_{i=1}^N \psi_{ki}^2 \right) \quad (7)$$

which represents approximate statistical independence between loss values  $L_i$  and feature components  $\psi_{ki}^2$  w.r.t. the distribution of data points  $\mathbf{x}_i$ .

In the rest of the paper we focus on analytical treatment of SGD dynamics in the SD approximation.

### 3 Reduction to generating functions

**Gas of rank-1 operators.** Note that iterations (4) are linear and can be compactly written as  $\Sigma_{t+1} = F_t \Sigma_t$  with a linear operator  $F_t$ . Assuming SD approximation (6), we only need to consider the diagonal parts in each of the four blocks of  $\Sigma$ . Then, the loss at time  $T$  can be expressed as

$$L(T) = \frac{1}{2} \text{Tr} \mathbf{H} \mathbf{C}_T = \frac{1}{2} \langle (\begin{smallmatrix} \lambda & 0 \\ 0 & 0 \end{smallmatrix}), F_T F_{T-1} \dots F_1 (\begin{smallmatrix} \mathbf{C}_0 & 0 \\ 0 & 0 \end{smallmatrix}) \rangle. \quad (8)$$

Here  $(\begin{smallmatrix} \lambda & 0 \\ 0 & 0 \end{smallmatrix}) = ((\begin{smallmatrix} \lambda_1 & 0 \\ 0 & 0 \end{smallmatrix}), (\begin{smallmatrix} \lambda_2 & 0 \\ 0 & 0 \end{smallmatrix}), \dots), (\begin{smallmatrix} \mathbf{C}_0 & 0 \\ 0 & 0 \end{smallmatrix}) = ((\begin{smallmatrix} C_{11,0} & 0 \\ 0 & 0 \end{smallmatrix}), (\begin{smallmatrix} C_{22,0} & 0 \\ 0 & 0 \end{smallmatrix}), \dots) \in \mathbb{R}^N \otimes \mathbb{R}^{2 \times 2}$  are  $(2 \times 2)$ -matrix-valued sequences indexed by the eigenvalues  $\lambda_k$ , and  $\langle \cdot, \cdot \rangle$  is the natural scalar product in  $l^2 \otimes \mathbb{R}^{2 \times 2}$ . The evolution operator  $F_t$  can be represented as the sum  $F_t = Q_t + A_t$  of a rank-one operator  $Q_t$  (noise term) and an operator  $A_t$  (noiseless term) that acts independently at each eigenvalue  $\lambda_k$  as a  $4 \times 4$  matrix:

$$Q_t = \gamma_t \alpha_t^2 \lambda (\begin{smallmatrix} 1 & 1 \\ 1 & 1 \end{smallmatrix}) \langle (\begin{smallmatrix} \lambda & 0 \\ 0 & 0 \end{smallmatrix}), \cdot \rangle, \quad (9)$$

$$A_t = (A_{t,\lambda}), \quad A_{t,\lambda} \Sigma = (\begin{smallmatrix} 1-\alpha_t \lambda & \beta_t \\ -\alpha_t \lambda & \beta_t \end{smallmatrix}) \Sigma (\begin{smallmatrix} 1-\alpha_t \lambda & \beta_t \\ -\alpha_t \lambda & \beta_t \end{smallmatrix})^T - \tau \gamma_t \alpha_t^2 \lambda^2 (\begin{smallmatrix} 1 & 0 \\ 1 & 0 \end{smallmatrix}) \Sigma (\begin{smallmatrix} 1 & 0 \\ 1 & 0 \end{smallmatrix})^T, \quad (10)$$

where  $\lambda = (\lambda_1, \lambda_2, \dots)^T$ . Let us expand the loss by the binomial formula, with  $m$  terms  $Q_t$  chosen at positions  $t_1, \dots, t_m$  and  $T - m$  terms  $A_t$  at the remaining positions:

$$L(T) = \frac{1}{2} \sum_{m=0}^T \sum_{0 < t_1 < \dots < t_m < T+1} U_{T+1, t_m} U_{t_m, t_{m-1}} \dots U_{t_2, t_1} V_{t_1}, \quad (11)$$

where

$$U_{t,s} = \langle (\begin{smallmatrix} \lambda & 0 \\ 0 & 0 \end{smallmatrix}), A_{t-1}A_{t-2} \cdots A_{s+1} \lambda (\begin{smallmatrix} 1 & 1 \\ 1 & 1 \end{smallmatrix}) \rangle \gamma_s \alpha_s^2, \quad (12)$$

$$V_t = \langle (\begin{smallmatrix} \lambda & 0 \\ 0 & 0 \end{smallmatrix}), A_{t-1}A_{t-2} \cdots A_1 (\begin{smallmatrix} C_0 & 0 \\ 0 & 0 \end{smallmatrix}) \rangle. \quad (13)$$

Expansion (11) has a suggestive interpretation as a partition function of a gas of rank-1 operators interacting with nearest neighbors (via  $U_{t,s}$ ) and the origin (via  $V_t$ ). Interactions via  $U_{t,s}$  contain the factor  $\gamma$  so that their strength depends on the sampling noise. We expect the model to be in different phases depending on the amount of noise: in the “signal-dominated” regime  $L(T)$  is primarily determined by  $V_t$  at large  $T$ , while in the “noise-dominated” regime  $L(T)$  is primarily determined by  $U_{t,s}$ . Below we show that such a phase transition indeed occurs for non-strongly convex problems.

**Generating functions.** Expansion (11) allows to compute  $L(T)$  iteratively:

$$L(T) = \frac{1}{2}V_{T+1} + \sum_{t_m=1}^T U_{T+1,t_m} L(t_m - 1). \quad (14)$$

For constant learning rates and momenta  $\alpha_t \equiv \alpha, \beta_t \equiv \beta$  we have  $F_t \equiv F$ , the value  $U_{t,s}$  becomes translation invariant,  $U_{t,s} = U_{t-s}$ , and the loss can be conveniently described by generating functions (or equivalently, Laplace transform):

$$\tilde{L}(z) = \sum_{t=0}^{\infty} L(t)z^t = \frac{\tilde{V}(z)/2}{1 - z\tilde{U}(z)}, \quad (15)$$

where  $\tilde{U}$  and  $\tilde{V}$  are the “noise” and “signal” generating functions:

$$\tilde{U}(z) = \sum_{t=0}^{\infty} U_{t+1}z^t = \gamma\alpha^2 \langle (\begin{smallmatrix} \lambda & 0 \\ 0 & 0 \end{smallmatrix}), (1 - zA)^{-1} \lambda (\begin{smallmatrix} 1 & 1 \\ 1 & 1 \end{smallmatrix}) \rangle \quad (16)$$

$$= \gamma\alpha^2 \sum_k \lambda_k^2 (\beta z + 1) / S(\alpha, \beta, \tau\gamma, \lambda_k, z), \quad (17)$$

$$\tilde{V}(z) = \sum_{t=0}^{\infty} V_{t+1}z^t = \langle (\begin{smallmatrix} \lambda & 0 \\ 0 & 0 \end{smallmatrix}), (1 - zA)^{-1} (\begin{smallmatrix} C_0 & 0 \\ 0 & 0 \end{smallmatrix}) \rangle \quad (18)$$

$$= \sum_k \lambda_k C_{kk,0} (2\alpha\beta\lambda_k z + \beta^3 z^2 - \beta^2 z - \beta z + 1) / S(\alpha, \beta, \tau\gamma, \lambda_k, z) \quad (19)$$

$$S(\alpha, \beta, \gamma, \lambda, z) = \alpha^2 \beta \gamma \lambda^2 z^2 + \alpha^2 \beta \lambda^2 z^2 + \alpha^2 \gamma \lambda^2 z - \alpha^2 \lambda^2 z - 2\alpha\beta^2 \lambda z^2 - 2\alpha\beta \lambda z^2 \\ + 2\alpha\beta \lambda z + 2\alpha \lambda z - \beta^3 z^3 + \beta^3 z^2 + \beta^2 z^2 - \beta^2 z + \beta z^2 - \beta z - z + 1.$$

In the remainder we derive various properties of the loss evolution by analyzing these formulas.

## 4 Convergence, phase transitions, parameter optimization, negative momenta

In this section, motivated by overparametrized neural networks, we assume a non-strongly-convex scenario with an infinite-dimensional and compact  $\mathbf{H}$ , i.e.,  $N = \infty$  and  $\lambda_k \rightarrow 0$ . Also we restrict ourselves to SD approximations with  $0 < \tau \leq 1$  as they seem to better fit practical problems like MNIST (see Figure 1 and Appendix E).

**Conditions of loss convergence (stability).** First note that as  $\lambda_k \rightarrow 0$  the “noiseless” components  $A_{\lambda_k}$  of the evolution operator  $F$  appearing in Eq. (10) have their action in trial matrix  $\Sigma$  converge to  $(\begin{smallmatrix} 1 & \beta \\ 0 & \beta \end{smallmatrix}) \Sigma (\begin{smallmatrix} 1 & \beta \\ 0 & \beta \end{smallmatrix})^T$ , and from (12) we get  $U_t = C \sum_k \lambda_k^2 (1 + o(1))$ . This means that if  $\sum_k \lambda_k^2 = \infty$  then  $U_t = \infty$  and loss diverges already at first step ( $L(t=1) = \infty$ ) – we call this effect *immediate divergence*. Next, assuming  $\sum_k \lambda_k^2 < \infty$ , loss stability can be related to the first positive singularity of the loss generating function  $\tilde{L}(z)$  given by (15). Indeed, let  $r_L$  be the convergence radius of power series (15). Since  $L(t) \geq 0$ ,  $\tilde{L}(z)$  must be monotone increasing on  $[0, r_L)$  and have a singularity at  $z = r_L$ . If  $r_L < 1$ , then  $L(t) \not\rightarrow 0$  as  $t \rightarrow \infty$ , while if  $r_L > 1$ , then  $L(t) \rightarrow 0$  exponentially fast. Thus, the condition of loss stability can be written as  $r_L \geq 1$ , which can be further related to the generating function  $\tilde{U}(z)$ .

**Proposition 3.** Let  $\beta \in (-1, 1)$ ,  $0 < \alpha < 2(\beta + 1)/\lambda_{\max}$  and  $\gamma \in [0, 1]$ . Then  $r_L < 1$  iff  $\tilde{U}(1) > 1$ .

This result is proved by showing that  $\tilde{U}(z), \tilde{V}(z)$  have no singularities for  $z \in (0, 1)$  and that  $z\tilde{U}(z)$  is monotone increasing on  $(0, 1)$ . The only source of singularity in  $\tilde{L}(z)$  is then the denominator in (15). Note that conditions  $\beta \in (-1, 1)$ ,  $0 < \alpha < 2(\beta + 1)/\lambda_{\max}$  exactly specify the convergence region for the non-stochastic problem with  $\gamma = 0$  (see [39, 45] and Appendix G). This is also a necessary condition in the presence of sampling noise since the second term in (4) is a positive semi-definite matrix.

Evaluating  $\tilde{U}(z)$  at  $z = 1$ , we find

$$\tilde{U}(1) = \sum_k \frac{\gamma\alpha\lambda_k(\beta + 1)}{\alpha\beta\tau\gamma\lambda_k + \alpha\beta\lambda_k + \alpha\tau\gamma\lambda_k - \alpha\lambda_k - 2\beta^2 + 2} = \frac{\alpha\gamma}{2(1 - \beta)} \sum_k \lambda_k(1 + O(\lambda_k)). \quad (20)$$

This shows that  $\sum_k \lambda_k = \infty$  iff  $\tilde{U}(1) = \infty > 1$  (regardless of values of  $\alpha, \beta, \gamma$ ), so that  $r_L < 1$  and  $L(t)$  diverges exponentially as  $t \rightarrow \infty$ . We call this situation *eventual divergence*.

We examine next the practically common case of momentum close to 1, when  $\delta := 1 - \beta \rightarrow 0+$ . From the first equality in (20) we get  $\tilde{U}(1) = \sum_k \frac{\lambda_k(1 + O(\alpha\lambda_k))}{\tau\lambda_k + 2\delta/(\alpha\gamma)}$ . Dropping the  $O(\alpha\lambda_k)$  term and assuming for simplicity that  $\tau = 1$ , we arrive at an approximate convergence condition which can be expressed in terms of the regularization parameter  $\lambda = \lambda_{\text{crit}}$  at which the “effective dimension”  $d_{\text{eff}} = \sum_k \lambda_k/(\lambda_k + \lambda)$  of  $\mathbf{H}$  equals 1:

$$\alpha_{\text{eff}}\gamma \lesssim \frac{2}{\lambda_{\text{crit}}}, \text{ where } \sum_k \frac{\lambda_k}{\lambda_k + \lambda_{\text{crit}}} = 1. \quad (21)$$

Both conditions (20), (21) agree very well with experiments on MNIST and synthetic data (Fig. 2).

**Exponential divergence.** Our stability analysis above shows that loss diverges at large  $t$  when  $\tilde{U}(1) > 1$ . This divergence is primarily characterized by the convergence radius  $r_L$  determined from the equation  $r_L\tilde{U}(r_L) = 1$  according to (15). Indeed, assuming an asymptotically exponential ansatz  $L(t) \sim Ce^{t/t_{\text{div}}}$ , we immediately get the divergence time scale  $t_{\text{div}} = -1/\log r_L$ . A closer inspection of  $\tilde{L}(z)$  near  $r_L$  also allows to determine the constant  $C$  (see appendix D.4):

$$L(t) \sim \frac{\tilde{V}(r_L)}{2(1 + r_L^2\tilde{U}'(r_L))} r_L^{-t}. \quad (22)$$

Note that  $r_L$  can be very close to 1, which is naturally observed in *eventual divergent* phase by taking sufficiently small  $\alpha$  and/or  $\gamma$ . In this case the characteristic divergence time  $t_{\text{div}}$  is large and we expect the exponential divergent behavior occur only for  $t \gtrsim t_{\text{blowup}}$ , while for  $t \ll t_{\text{blowup}}$  the loss converges roughly with the rate of noiseless model  $\tilde{U}(z) \equiv 0$ . As  $t_{\text{blowup}}$  should have a meaning of a time moment where loss starts to significantly deviate from noiseless trajectory we define it by equating divergent (22) and noiseless losses. We confirm these effects experimentally in Figure 3 (right).

**Power laws and two convergence regimes.** Note that if  $\lambda_k \rightarrow 0$  and  $C_{kk,0} > 0$  for infinitely many  $k$ , then  $r_L \leq 1$ , thus excluding the possibility of exponential loss convergence. Indeed,  $S(\alpha, \beta, \gamma, \lambda, z) \xrightarrow{\lambda \rightarrow 0} (1 - z)(1 - \beta z)(1 - \beta^2 z)$ . It follows that for small  $\lambda_k$  the respective terms in expansion (17) have three poles  $z_{k,0}, z_{k,1}, z_{k,2}$  converging to  $1, \beta^{-1}, \beta^{-2}$ , respectively. By Eq. (15),  $\tilde{L}(z)$  has a removable singularity at  $z_{k,0}$ , moreover  $\tilde{L}(z_{k,0}) < 0$  if  $C_{kk,0} > 0$  and  $k$  is large enough, meaning that  $r_L < z_{k,0}$ . We then get  $r_L \leq 1$  by taking the limit in  $k$ .

To get a more detailed picture of the loss evolution let us assume now that the eigenvalues  $\lambda_k$  and the second moments  $C_{kk,0}$  of initial ( $t = 0$ ) approximation error are subject to large- $k$  power laws

$$\lambda_k = \Lambda k^{-\nu}(1 + o(1)), \quad \sum_{l \geq k} \lambda_l C_{ll,0} = K k^{-\varkappa}(1 + o(1)) \quad (23)$$

with some exponents  $\nu, \varkappa > 0$  (also denote  $\zeta = \varkappa/\nu$ ) and coefficients  $\Lambda, K$ . Such (or similar) power laws are empirically observed in many high-dimensional problems ([12, 2, 29, 10, 27, 14, 1, 7, 3, 6])

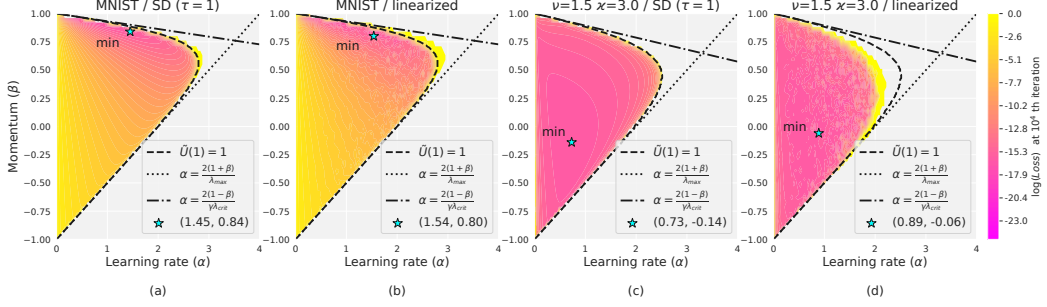


Figure 2:  $L(t = 10^4)$  for different learning rates  $\alpha$  and momenta  $\beta$ , in the SD( $\tau = 1$ ) and linearized regimes, for MNIST and synthetic data given by Eq. (23) with  $\nu = 1.5$ ,  $\kappa = 3$ , for  $b = 10$ . Black lines show convergence boundaries from Proposition (3) and Eqs. (20) and (21). MNIST experiment is in the signal-dominated phase and synthetic in the noise-dominated. The stars show  $\arg \min_{\alpha, \beta} L$ .

and Figure 1), can be derived theoretically [3, 48], and are often assumed for theoretical optimization guarantees [33, 9, 19, 20, 17, 47, 11, 43, 5, 53]. If  $\nu \leq \frac{1}{2}$ , then  $\sum_k \lambda_k^2 = \infty$  and we are in the “immediate divergence” regime mentioned earlier, and if  $\frac{1}{2} < \nu \leq 1$ , then  $\sum_k \lambda_k = \infty$  and we are in “eventual divergence” regime. Away from these two divergent regimes, we precisely characterize the late time loss asymptotics:

**Theorem 1.** Assume spectral conditions (23) with  $\nu > 1$  and that parameters  $\alpha, \beta, \gamma$  are as in Proposition 3 and such that convergence condition  $\tilde{U}(1) < 1$  is satisfied. Then

$$\sum_{t=1}^T tL(t) = (1 + o(1)) \begin{cases} \frac{K\Gamma(\zeta+1)}{2(1-\tilde{U}(1))(2-\zeta)} \left(\frac{2\alpha\Lambda}{1-\beta}\right)^{-\zeta} t^{2-\zeta}, & 2-\zeta > 1/\nu, \\ \frac{\gamma\tilde{V}(1)\Gamma(2-1/\nu)}{8(1-\tilde{U}(1))^2} \left(\frac{2\alpha\Lambda}{1-\beta}\right)^{1/\nu} t^{1/\nu}, & 2-\zeta < 1/\nu. \end{cases} \quad (24)$$

The idea of the proof is to 1) observe by Proposition 3 that  $r_L = 1$ ; 2) show that for  $z = 1 - \varepsilon$  close to the singularity  $z = 1$  the derivative  $\frac{d}{dz} \tilde{L}(z) = \sum_{t=1}^{\infty} tL(t)z^{t-1}$  of the loss generating function diverges as  $\frac{d}{dz} \tilde{L}(1 - \varepsilon) \propto \varepsilon^{\zeta-2}$ ; 3) apply the Tauberian theorem to relate the asymptotic  $\frac{d}{dz} \tilde{L}(1 - \varepsilon) \approx C\varepsilon^{\zeta-2}$  to the asymptotic of the partial sum  $\sum_t^T tL(t) \approx \frac{C}{\Gamma(3-\zeta)} T^{2-\zeta}$ . The second step can be done by writing

$$\frac{d}{dz} \tilde{L}(z) = \frac{\frac{d}{dz} \tilde{V}(z)}{2(1 - z\tilde{U}(z))} + \frac{\tilde{V}(z) \frac{d}{dz} (z\tilde{U}(z))}{2(1 - z\tilde{U}(z))^2} \quad (25)$$

One can then show using (17), (18) that  $\tilde{U}'(z)$  diverges as  $\tilde{U}'(1 - \varepsilon) \propto \varepsilon^{-\frac{1}{\nu}}$  and  $\tilde{V}'(z)$  diverges as  $\tilde{V}'(1 - \varepsilon) \propto \varepsilon^{\zeta-2}$  for  $\zeta < 2$ . Depending on which of the two terms dominates in Eq. (25) at small  $\varepsilon$ , we observe two qualitatively different phases (previously known in SGD without momenta [47]): the “signal-dominated” phase at  $\zeta - 2 < 1/\nu$  and the “noise-dominated” phase at  $\zeta - 2 > 1/\nu$ .

In the sequel we will assume that not only the cumulative sums  $\sum_1^T tL(t)$ , but also the individual values  $L(t)$  obey a power-law  $L(t) \propto t^{-\zeta}$ . Then from (24) we immediately get

$$L(t) = (1 + o(1)) \begin{cases} \frac{K\Gamma(\zeta+1)}{2(1-\tilde{U}(1))} \left(\frac{2\alpha\Lambda}{1-\beta}\right)^{-\zeta} t^{-\zeta}, & \zeta < 2 - 1/\nu, \end{cases} \quad (26a)$$

$$\begin{cases} \frac{\gamma\tilde{V}(1)\Gamma(2-1/\nu)}{8\nu(1-\tilde{U}(1))^2} \left(\frac{2\alpha\Lambda}{1-\beta}\right)^{1/\nu} t^{1/\nu-2}, & \zeta > 2 - 1/\nu. \end{cases} \quad (26b)$$

See Figure 3(left) for the resulting full phase diagram.

**Transitions between phases.** Explicit result (24) allow us to go further in understanding the “noise-dominated” phase  $\zeta > 2 - 1/\nu$ . Representation (25) and linearity of Laplace transform allows to write loss asymptotic as  $L(t) \approx C_{\text{signal}} t^{-\zeta} + C_{\text{noise}} t^{-2+\frac{1}{\nu}}$  with two terms given by (26a), (26b). As  $C_{\text{noise}}$  vanishes in the noiseless limit  $\gamma \rightarrow 0$ , we expect that for sufficiently small  $\gamma$  the signal term here dominates the noise term up to time scale  $t_{\text{trans}}$  given by

$$t_{\text{trans}} = \left( \frac{C_{\text{signal}}}{C_{\text{noise}}} \right)^{1/(\zeta-2+1/\nu)} = \left( \frac{(1-\beta)}{2\alpha\Lambda} \right)^{1/\nu+\zeta} \frac{4\nu K\Gamma(\zeta+1)(1-\tilde{U}(1))}{\gamma\Gamma(2-1/\nu)\tilde{V}(1)}^{1/(\zeta-2+1/\nu)}. \quad (27)$$

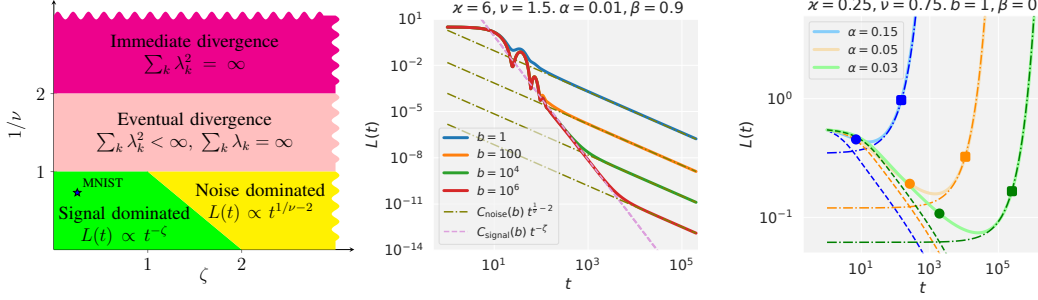


Figure 3: **Left:** Phase diagram for  $L(t)$  under power-law spectral conditions (23). **Center:** Transition from signal-dominated to noise-dominated regime during model training. Asymptotic power-law lines are calculated from (26a) and (26b). **Right:** Divergent  $L(t)$  in the phase  $\frac{1}{2} < \nu < 1$ : experimental trajectories (solid) with marked points at positions  $t = t_{\text{div}}$  (squares) and  $t = t_{\text{blowup}}$  (circles), theoretical late-time asymptotics (22) (dash-dotted) and noiseless early time trajectories (dashed).

This conclusion is fully confirmed by our experiments with simulated data, see Figure 3(center). Note that the time scale  $t_{\text{trans}}$  can vary widely depending on  $\alpha, \beta, \gamma$ ; in particular,  $t_{\text{trans}}$  might not be reached at all in realistic optimization time if the noise  $\gamma$  and effective learning rate  $\frac{\alpha}{1-\beta}$  are small.

A similar reasoning can be used to estimate the time  $t_{\text{blowup}}$  of transition from early convergence to subsequent divergence (see Figure 3 (right)). In Section D.4 we consider the scenario with  $\beta = 0, \gamma = \tau = 1$  and power laws (23) in which  $\frac{1}{2} < \nu < 1$  (eventual divergence) and  $\zeta < 1$ . We show that at small learning rates  $\alpha$  we have  $t_{\text{blowup}} \approx a_* t_{\text{div}} \approx a_* \left( \frac{1}{4\nu} \Gamma(2-1/\nu) \Gamma(1/\nu-1) \right)^{\nu/(\nu-1)} (2\alpha\Lambda)^{1/(\nu-1)}$ , where  $a_*$  is the solution of the equation  $\frac{1/\nu-1}{\Gamma(1-\zeta)} a_*^{-\zeta} = e^{a_*}$  and it depends only on  $\nu, \zeta$ .

**Hyperparameter and budget optimization.** The two natural concepts of budget in our setting are the *time budget*  $T$  (the total number of iterations) and the *computation budget*  $bT$ . We discuss now minimization of the loss value for available budgets. It is convenient to consider separately the two phases and assume that  $T$  is large enough for the asymptotic formulas (26a),(26b) to be applicable. Note that near the divergence boundary  $\tilde{U}(1) = 1$  the loss is high due to denominator  $1 - \tilde{U}(1)$  in Eqs. (26a),(26b). This suggests that at optimal  $\alpha, \beta$  the difference  $\tilde{U}(1) - 1$  is of order 1, which allows us to neglect dependence of loss on  $\tilde{U}(1)$  as long as convergence condition  $\tilde{U}(1) < 1$  is satisfied.

*“Signal-dominated” phase* ( $\zeta < 2-1/\nu$ ). By Eq. (26a),  $L(t) \gtrsim C(\alpha_{\text{eff}} t)^{-\zeta}$  with a problem-dependent constant  $C$ . Thus to minimize  $L(t)$  for a fixed time budget  $t$ , we need to maximize  $\alpha_{\text{eff}}$ . However, we are limited by convergence condition (21) stating that  $\alpha_{\text{eff}} \lesssim \frac{2}{\lambda_{\text{crit}} \gamma}$ , and implying in particular that  $L(t) \gtrsim C' \gamma^\zeta t^{-\zeta}$ . Since  $\gamma$  is determined by the batch size (see Proposition 1), once the batch size is limited, we get a general lower bound on the asymptotic of  $L(t)$  that cannot be improved by any adjustment of  $\alpha, \beta$ . This contrasts markedly with the non-stochastic GD ( $\gamma = 0$ ), in which one can improve loss convergence by bringing  $\beta$  arbitrarily close to 1 and hence making  $\alpha_{\text{eff}}$  arbitrarily large [33, 16]. See the two left subplots in Figure 2 for an illustration on MNIST.

Recalling that  $\gamma \approx \frac{1}{b}$  for  $N \gg b$ , we see that at the optimal  $\alpha_{\text{eff}}$  the loss  $L(t) \approx C'(bt)^{-\zeta}$ , i.e. it is (approximately) a function of the total computation budget regardless of its distribution over iterations and batchsizes. This conclusion agrees with existing results on approximately linear scalability of SGD with batch size [30, 41]. (We remark that this scalability breaks down at larger batch sizes; there is no contradiction with above power law since Eq. (26a) and hence the power law are established for  $t \rightarrow \infty$ ). See Fig. 5 in Appendix for an illustration on MNIST.

*“Noise-dominated” phase* ( $\zeta > 2-1/\nu$ ). Here Eq. (26b) implies  $L(t) \approx C\gamma\tilde{V}(1)\alpha_{\text{eff}}^{1/\nu} t^{1/\nu-2}$ . We see in particular that  $\alpha_{\text{eff}}$  appears with the *positive* power  $1/\nu$ , so that (in contrast to the signal-dominated scenario) high effective learning rates are disadvantageous. At the same time, it can be shown that  $\tilde{V}(1) \propto \frac{1}{\alpha}$  at small  $\alpha$ , so it is neither favorable to use small  $\alpha$ . Experiments with synthetic data in the noise-dominated regime in Fig. 2 show that the loss is indeed minimized when both  $\alpha$  is kept away from 0 and  $\alpha_{\text{eff}}$  from the maximum admissible value  $\frac{2}{\lambda_{\text{crit}} \gamma}$ .



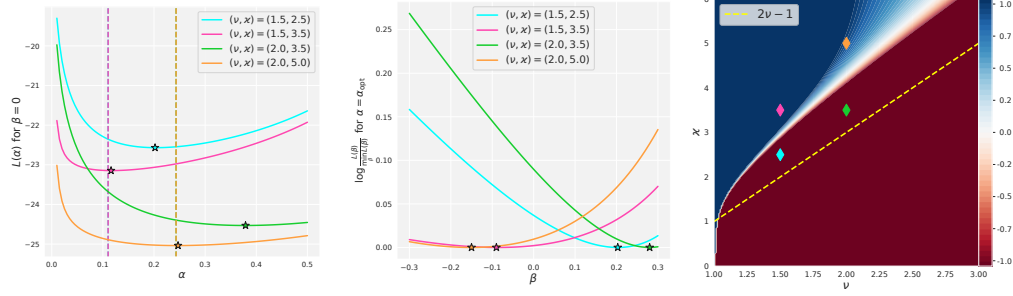


Figure 4: **Left:** Dependence of the loss  $L(t = 10^4)$  on the learning rate  $\alpha$  at  $\beta = 0$ , for several synthetic datasets (23) at different  $\nu$  and  $\varkappa$  in the “noisy” phase. The stars show the empirically determined optimal learning rates  $\arg \min_{\alpha} L(\alpha)$ , and the dashed lines show the theoretical values  $\alpha_{\text{opt}} = (\sum_k \lambda_k)^{-1} \frac{2(\nu-1)}{3\nu-1}$ . The empirical results match the theory for the points  $(\nu, \varkappa) = (1.5, 3.5)$  and  $(\nu, \varkappa) = (2.0, 5.0)$  that are deep in the noisy phase so that the loss is represented well by theoretical asymptotic (26b). In contrast, the points  $(\nu, \varkappa) = (1.5, 2.5)$  and  $(\nu, \varkappa) = (2.0, 3.5)$  are close to the phase boundary, and the loss term  $C_{\text{signal}} t^{-\zeta}$  representing the competing phase is too large for them to be neglected, explaining the discrepancy with the theoretical estimate. **Center:** Dependence of the loss log-ratio  $\log \frac{L(\beta)}{\min_{\beta} L(\beta)}$  on  $\beta$  at experimental  $\alpha_{\text{opt}}$ . The stars show  $\arg \min_{\beta} L(\beta)$ . In two scenarios the minimum is attained at  $\beta < 0$ , and in the other two at  $\beta > 0$ . **Right:** The value (28) theoretically characterizing improvement from decreased momenta  $\beta < 0$  at large  $t$  by Proposition 7, computed for the range  $(\nu, \varkappa) \in [1, 3] \times [0, 6]$  of power-law models (23). The diamonds show the pairs  $(\nu, \varkappa)$  in the experiments on the left and central figures. In agreement with the theoretical prediction, the value (28) is positive in those scenarios where the optimal  $\beta$  is negative, and vice versa. The dashed yellow line  $\varkappa = 2\nu - 1$  separates the signal-dominated and the noise-dominated regimes; the four performed experiments belong to the noise-dominated regime.

**Negative momenta.** It is known that in some noisy settings momenta  $\beta > 0$  do not improve convergence compared to  $\beta = 0$  [36, 24]. We show now that in our noise-dominated regime the optimal configuration of  $\alpha, \beta$  may be achieved with a *negative* momentum  $\beta$  (two right subplots in Fig. 2). To clarify this effect, assume that approximation (26b) is applicable and can be differentiated w.r.t.  $\alpha$  and  $\beta$ . Assume also that  $\gamma = 1$  (this allows to simplify some formulas). Then, by computing  $\partial_{\alpha} L(t)|_{\beta=0}$  using approximation (26b), it can be shown that  $L(t)|_{\beta=0}$  is minimized at  $\alpha = \alpha_{\text{opt}} \approx (\sum_k \lambda_k)^{-1} \frac{2(\nu-1)}{3\nu-1}$ . Now we compute  $\partial_{\beta} L(t)|_{\beta=0, \alpha=\alpha_{\text{opt}}}$  and find that its sign is equal to the sign of the expression

$$\nu \sum_k \lambda_k \sum_k \lambda_k C_{kk,0} - (\nu - 1) \sum_k \lambda_k^2 \sum_k C_{kk,0}. \quad (28)$$

It follows that if this expression is positive, then configuration  $(\alpha_{\text{opt}}, \beta)$  with a small negative  $\beta$  provides a lower loss than any configuration with  $\beta = 0$ . We find a good agreement of this conclusion with experiment (Figure 4).

Interestingly, we do not observe (both experimentally and theoretically) this effect for the signal-dominated phase. Retracing above steps with Eq. (26b) replaced by Eq. (26a), we find  $\partial_{\beta} L(t)|_{\beta=0, \alpha=\alpha_{\text{opt}}}$  to be always negative. We conclude that in the signal-dominated phase the loss is minimized at  $\beta > 0$ . See Appendix D.6 and Proposition 7 there for details.

## 5 Conclusion

In this work we have proposed a two step framework which allowed us to get a precise characterization of mini-batch SGD dynamics with momentum. In the first step we performed a *spectral diagonal* approximation for the exact dynamics of the second moments of model weights. This approximation makes the dynamics tractable and is even exact in a number of scenarios. In the second step we developed a formalism based on generating functions that clearly distinguishes the roles of noiseless part and sampling noise in the overall SGD evolution, and also has a good quantitative agreement

with experiments. Finally, we applied the formalism to SGD with constant parameters (learning rate, momentum and batch size) and non-strongly convex problems to answer several questions including convergence conditions, different phases and transitions between them, and optimal SGD settings.

One of the prospective direction for future work is to find under which conditions on model and data the spectral diagonal approximation accurately describes the actual SGD. Next direction is to apply the developed formalism to problems with other spectral distributions, i.e. strongly convex. Another question is how loss fluctuates around its mean value, as in this work we focused on the loss averaged over sampling noise. Finally, it is interesting whether current approach can be extended to accelerated or adaptive version of SGD.

## The code

The code to reproduce experiments described in the paper can be found in the github repository <https://github.com/Godofnothing/PowerLawOptimization>.

## Acknowledgment

Research was supported by Russian Science Foundation, grant 21-11-00373. The authors acknowledge the use of computational resources of Skoltech computational cluster Zhores [51] for obtaining the results presented in this paper.

## 6 References

- [1] Alexander Atanasov, Blake Bordelon, and Cengiz Pehlevan. Neural networks as kernel learners: The silent alignment effect. *arXiv preprint arXiv:2111.00034*, 2021.
- [2] Yasaman Bahri, Ethan Dyer, Jared Kaplan, Jaehoon Lee, and Utkarsh Sharma. Explaining neural scaling laws. *arXiv preprint arXiv:2102.06701*, 2021.
- [3] Ronen Basri, Meirav Galun, Amnon Geifman, David Jacobs, Yoni Kasten, and Shira Kritchman. Frequency bias in neural networks for input of non-uniform density. In *International Conference on Machine Learning*, pages 685–694. PMLR, 2020.
- [4] Saugata Basu. Algorithms in real algebraic geometry: a survey. *arXiv preprint arXiv:1409.1534*, 2014.
- [5] Raphaël Berthier, Francis Bach, and Pierre Gaillard. Tight nonparametric convergence rates for stochastic gradient descent under the noiseless linear model. *arXiv preprint arXiv:2006.08212*, 2020.
- [6] Alberto Bietti. Approximation and learning with deep convolutional models: a kernel perspective. *arXiv preprint arXiv:2102.10032*, 2021.
- [7] Blake Bordelon and Cengiz Pehlevan. Learning curves for sgd on structured features. *arXiv preprint arXiv:2106.02713*, 2021.
- [8] Léon Bottou and Olivier Bousquet. The tradeoffs of large scale learning. In J. Platt, D. Koller, Y. Singer, and S. Roweis, editors, *Advances in Neural Information Processing Systems*, volume 20. Curran Associates, Inc., 2007.
- [9] Helmut Brakhage. On ill-posed problems and the method of conjugate gradients. In *Inverse and ill-posed Problems*, pages 165–175. Elsevier, 1987.
- [10] Abdulkadir Canatar, Blake Bordelon, and Cengiz Pehlevan. Spectral bias and task-model alignment explain generalization in kernel regression and infinitely wide neural networks. *Nature Communications*, 12(1), may 2021.
- [11] Andrea Caponnetto and Ernesto De Vito. Optimal rates for the regularized least-squares algorithm. *Foundations of Computational Mathematics*, 7(3):331–368, 2007.
- [12] Hugo Cui, Bruno Loureiro, Florent Krzakala, and Lenka Zdeborová. Generalization error rates in kernel regression: The crossover from the noiseless to noisy regime. *Advances in Neural Information Processing Systems*, 34, 2021.

- [13] Andreas Dolzmann and Thomas Sturm. Redlog: Computer algebra meets computer logic. *Acm Sigsum Bulletin*, 31(2):2–9, 1997.
- [14] Xialiang Dou and Tengyuan Liang. Training neural networks as learning data-adaptive kernels: Provable representation and approximation benefits. *Journal of the American Statistical Association*, 116(535):1507–1520, apr 2020.
- [15] William Feller. *An introduction to probability theory and its applications. Vol. II.* Second edition. John Wiley & Sons Inc., New York, 1971.
- [16] Nicolas Flammarion and Francis Bach. From averaging to acceleration, there is only a step-size. In *Conference on Learning Theory*, pages 658–695. PMLR, 2015.
- [17] Sergei Farshatovich Gilyazov and Nataliâ L’vovna Gol’dman. *Regularization of ill-posed problems by iteration methods*, volume 499. Springer Science & Business Media, 2013.
- [18] Ian Goodfellow, Yoshua Bengio, and Aaron Courville. *Deep Learning*. MIT Press, 2016. <http://www.deeplearningbook.org>.
- [19] Martin Hanke. Accelerated landweber iterations for the solution of ill-posed equations. *Numerische mathematik*, 60(1):341–373, 1991.
- [20] Martin Hanke. Asymptotics of orthogonal polynomials and the numerical solution of ill-posed problems. *Numerical Algorithms*, 11(1):203–213, 1996.
- [21] Nicholas JA Harvey, Christopher Liaw, Yaniv Plan, and Sikander Randhawa. Tight analyses for non-smooth stochastic gradient descent. In *Conference on Learning Theory*, pages 1579–1613. PMLR, 2019.
- [22] Arthur Jacot, Franck Gabriel, and Clément Hongler. Neural tangent kernel: Convergence and generalization in neural networks. *arXiv preprint arXiv:1806.07572*, 2018.
- [23] Prateek Jain, Dheeraj Nagaraj, and Praneeth Netrapalli. Making the last iterate of sgd information theoretically optimal. In *Conference on Learning Theory*, pages 1752–1755. PMLR, 2019.
- [24] Rahul Kidambi, Praneeth Netrapalli, Prateek Jain, and Sham Kakade. On the insufficiency of existing momentum schemes for stochastic optimization. In *2018 Information Theory and Applications Workshop (ITA)*, pages 1–9. IEEE, 2018.
- [25] Jack Kiefer and Jacob Wolfowitz. Stochastic estimation of the maximum of a regression function. *The Annals of Mathematical Statistics*, pages 462–466, 1952.
- [26] Hermann König. *Eigenvalue distribution of compact operators*, volume 16. Birkhäuser, 2013.
- [27] Dmitry Kopitkov and Vadim Indelman. Neural spectrum alignment: Empirical study. In *International Conference on Artificial Neural Networks*, pages 168–179. Springer, 2020.
- [28] Yann LeCun, Yoshua Bengio, and Geoffrey Hinton. Deep learning. *nature*, 521(7553):436–444, 2015.
- [29] Jaehoon Lee, Samuel Schoenholz, Jeffrey Pennington, Ben Adlam, Lechao Xiao, Roman Novak, and Jascha Sohl-Dickstein. Finite versus infinite neural networks: an empirical study. *Advances in Neural Information Processing Systems*, 33:15156–15172, 2020.
- [30] Siyuan Ma, Raef Bassily, and Mikhail Belkin. The power of interpolation: Understanding the effectiveness of sgd in modern over-parametrized learning. In *International Conference on Machine Learning*, pages 3325–3334. PMLR, 2018.
- [31] Aaron Meurer, Christopher P. Smith, Mateusz Paprocki, Ondřej Čertík, Sergey B. Kirpichev, Matthew Rocklin, AMiT Kumar, Sergiu Ivanov, Jason K. Moore, Sartaj Singh, Thilina Rathnayake, Sean Vig, Brian E. Granger, Richard P. Muller, Francesco Bonazzi, Harsh Gupta, Shivam Vats, Fredrik Johansson, Fabian Pedregosa, Matthew J. Curry, Andy R. Terrel, Štěpán Roučka, Ashutosh Saboo, Isuru Fernando, Sumith Kulal, Robert Cimrman, and Anthony Scopatz. Sympy: symbolic computing in python. *PeerJ Computer Science*, 3:e103, January 2017.
- [32] Eric Moulines and Francis Bach. Non-asymptotic analysis of stochastic approximation algorithms for machine learning. *Advances in neural information processing systems*, 24, 2011.
- [33] Arkadi S Nemirovskiy and Boris T Polyak. Iterative methods for solving linear ill-posed problems under precise information. *Eng. Cyber.*, (4):50–56, 1984.

- [34] Yurii Evgen'evich Nesterov. A method of solving a convex programming problem with convergence rate  $o(k^2)$ . In *Doklady Akademii Nauk*, volume 269, pages 543–547. Russian Academy of Sciences, 1983.
- [35] Boris T Polyak. Some methods of speeding up the convergence of iteration methods. *Ussr computational mathematics and mathematical physics*, 4(5):1–17, 1964.
- [36] B.T. Polyak. *Introduction to Optimization*. Optimization Software, New York, 1987.
- [37] John Proakis. Channel identification for high speed digital communications. *IEEE Transactions on Automatic Control*, 19(6):916–922, 1974.
- [38] Herbert Robbins and Sutton Monro. A stochastic approximation method. *The annals of mathematical statistics*, pages 400–407, 1951.
- [39] Sumit Roy and John J Shynk. Analysis of the momentum lms algorithm. *IEEE transactions on acoustics, speech, and signal processing*, 38(12):2088–2098, 1990.
- [40] David E Rumelhart, Geoffrey E Hinton, and Ronald J Williams. Learning representations by back-propagating errors. *nature*, 323(6088):533–536, 1986.
- [41] Christopher J Shallue, Jaehoon Lee, Joseph Antognini, Jascha Sohl-Dickstein, Roy Frostig, and George E Dahl. Measuring the effects of data parallelism on neural network training. *arXiv preprint arXiv:1811.03600*, 2018.
- [42] Ohad Shamir and Tong Zhang. Stochastic gradient descent for non-smooth optimization: Convergence results and optimal averaging schemes. In Sanjoy Dasgupta and David McAllester, editors, *Proceedings of the 30th International Conference on Machine Learning*, volume 28 of *Proceedings of Machine Learning Research*, pages 71–79, Atlanta, Georgia, USA, 17–19 Jun 2013. PMLR.
- [43] Ingo Steinwart, Don R Hush, Clint Scovel, et al. Optimal rates for regularized least squares regression. In *COLT*, pages 79–93, 2009.
- [44] Ilya Sutskever, James Martens, George Dahl, and Geoffrey Hinton. On the importance of initialization and momentum in deep learning. In *International conference on machine learning*, pages 1139–1147. PMLR, 2013.
- [45] Mehmet Ali Tugay and Yalcin Tanik. Properties of the momentum lms algorithm. *Signal Processing*, 18(2):117–127, 1989.
- [46] Aditya Varre and Nicolas Flammarion. Accelerated sgd for non-strongly-convex least squares. *arXiv preprint arXiv:2203.01744*, 2022.
- [47] Aditya Varre, Loucas Pillaud-Vivien, and Nicolas Flammarion. Last iterate convergence of sgd for least-squares in the interpolation regime. *arXiv preprint arXiv:2102.03183*, 2021.
- [48] Maksim Velikanov and Dmitry Yarotsky. Explicit loss asymptotics in the gradient descent training of neural networks. *Advances in Neural Information Processing Systems*, 34, 2021.
- [49] Jingfeng Wu, Wenqing Hu, Haoyi Xiong, Jun Huan, Vladimir Braverman, and Zhanxing Zhu. On the noisy gradient descent that generalizes as sgd. In *International Conference on Machine Learning*, pages 10367–10376. PMLR, 2020.
- [50] Kun Yuan, Bicheng Ying, and Ali H Sayed. On the influence of momentum acceleration on online learning. *The Journal of Machine Learning Research*, 17(1):6602–6667, 2016.
- [51] I. Zacharov, R. Arslanov, M. Gunin, D. Stefonishin, A. Bykov, S. Pavlov, O. Panarin, A. Maliutin, S. Rykovanov, and M. Fedorov. Zhores - petaflops supercomputer for data-driven modeling, machine learning and artificial intelligence installed in skolkovo institute of science and technology. In *Open Engineering*, volume 9(1), pages 512–520, 2019.
- [52] Zhanxing Zhu, Jingfeng Wu, Bing Yu, Lei Wu, and Jinwen Ma. The anisotropic noise in stochastic gradient descent: Its behavior of escaping from sharp minima and regularization effects. *arXiv preprint arXiv:1803.00195*, 2018.
- [53] Difan Zou, Jingfeng Wu, Vladimir Braverman, Quanquan Gu, and Sham M Kakade. Benign overfitting of constant-stepsizes sgd for linear regression. *arXiv preprint arXiv:2103.12692*, 2021.

## Contents

<b>1</b>	<b>Introduction</b>	<b>1</b>
<b>2</b>	<b>The setting and the <i>Spectral Diagonal</i> approximation</b>	<b>3</b>
<b>3</b>	<b>Reduction to generating functions</b>	<b>4</b>
<b>4</b>	<b>Convergence, phase transitions, parameter optimization, negative momenta</b>	<b>5</b>
<b>5</b>	<b>Conclusion</b>	<b>9</b>
<b>6</b>	<b>References</b>	<b>10</b>
<b>A</b>	<b>Related work</b>	<b>14</b>
<b>B</b>	<b>Details of the setting</b>	<b>15</b>
B.1	Basics . . . . .	15
B.2	Eigendecompositions and other details . . . . .	15
B.3	Output and parameter spaces . . . . .	17
<b>C</b>	<b>Dynamics of second moments</b>	<b>18</b>
C.1	Derivation of second moments dynamic equation . . . . .	18
C.2	Translation invariant models . . . . .	21
<b>D</b>	<b>Generating functions and their applications</b>	<b>22</b>
D.1	Reduction to generating functions . . . . .	22
D.2	Convergence conditions . . . . .	22
D.3	Loss asymptotic under power-laws . . . . .	24
D.4	Exponential divergence of the loss and convergence-divergence transition . . . . .	27
D.5	Budget optimization . . . . .	30
D.6	Negative momenta . . . . .	30
<b>E</b>	<b>Experiments</b>	<b>32</b>
E.1	Training regimes . . . . .	32
E.2	Datasets . . . . .	33
E.3	Experimental details . . . . .	33
E.4	Additional experiments . . . . .	34
E.5	Validity of spectral diagonal approximation . . . . .	34
<b>F</b>	<b>Mini-batch SGD vs. SGD with additive noise</b>	<b>36</b>
<b>G</b>	<b>Noiseless convergence condition</b>	<b>36</b>

## A Related work

**SGD.** Stochastic Gradient Descent (SGD) was introduced in [38], and its various versions have been extensively studied since then, see e.g. [25, 40, 8, 42, 23, 21, 32]. The version (1) considered in the present paper is motivated by applications to training neural networks and is widely used [28, 18, 44]. Its key feature is the presence of momentum, which is both theoretically known to improve convergence and widespread in practice [35, 36, 34, 44, 41].

**Mini-batch SGD and spectral diagonal representation.** In the present paper we consider the *mini-batch* SGD, meaning that the stochasticity in SGD is specifically associated with the random choice of different batches used to approximate the full loss function at each iteration (not to be confused with SGD modeled as gradient descent with additive noise as e.g. in the gradient Langevin dynamics; see e.g. [49, 52] for some discussion and comparison, as well as our Section F for an illustration in our case of quadratic problems). We study this SGD in terms of how the second moments of the errors evolve with time. Our Proposition 1 generalizes existing evolution equations [47] to SGD with momentum. A serious difficulty in the study of this evolution is the presence of higher order mixing terms coupling different spectral components (the first term on the r.h.s. in our Eq. (5)). In [47], it was shown that the effects of these terms can be controlled by suitable inequalities, allowing to establish upper bounds on error rates. Our approach is different and is close to the approach of recent paper [7]: we rather *assume* that the full evolution can be replaced by what we call *Spectral Diagonal* approximation (see Section 2 for details and discussion). We consider a family of such approximations parameterized by scalar  $\tau$ , while [7] considers a particular case (in our notation,  $\tau = -1$ ). The SD assumption allows us to go beyond upper bounds and obtain explicit coefficients in the asymptotics of large- $t$  loss evolution (see Theorem 1).

**Spectral power laws.** In Section 4 we adopt at some point very convenient *power law spectral assumptions* (23) on the asymptotic behavior of eigenvalues and target expansion coefficients. Such power laws are empirically observed in many high-dimensional problems [12, 2, 29, 10, 27, 14, 1, 7, 3, 6], can be derived theoretically [3, 48], and closely related conditions are often assumed for theoretical optimization guarantees [33, 9, 19, 20, 17, 47, 11, 43, 5, 53]. An important aspect of our work is that, in contrast to most other works, we allow the exponent  $\zeta$  characterizing initial second moments  $C_{kk,0}$  to have values in the interval  $(0, 1)$ . In this case,  $\sum_k \lambda_k C_{kk} < \infty$  while  $\sum_k C_{kk,0} = \infty$ . This effectively means that the target function  $y^*(\mathbf{x})$  has a finite euclidean norm, while the norm of the respective optimal weight vector  $\mathbf{w}^*$  is infinite (i.e., the loss does not have a minimum). This broader assumption allows us, in particular, to correctly describe the loss evolution on MNIST for which  $\zeta \approx 0.25$  (see Figures 1 and 3): without assuming  $\|\mathbf{w}^*\| = \infty$ , the SGD is proved to have error rate  $O(t^{-\xi})$  with  $\xi \geq 1$  [47], which clearly contradicts the experiment (see Figure 1(left)).

**Phase diagram.** It is known that performance of SGD can be decomposed into “bias” and “variance” terms, with the dominant term determining what we call “signal-dominated” or “noise-dominated” regime [32, 47, 46]. In particular, see [47] for respective upper bounds for SGD without momentum. The main novelty of our paper compared to these previous results is the analytic framework allowing to obtain large- $t$  loss asymptotics with explicit constants for SGD with momentum (see Theorem 1) and use them to derive various quantitative conclusions related to model stability, phase transitions, and parameter optimization (see Section 4).

**Noisy GD with momentum.** GD with momentum (Heavy Ball) [35] was extensively studied, but mostly in a noiseless setting or for generic (non-sampling) kinds of noise; see e.g. the monograph [36]. See [37, 39, 45] for a discussion of stability on quadratic problems. [36] analyses various methods with noisy gradients for different kinds of noise and concludes that the fast convergence advantage of Heavy Ball and Conjugate Gradients (compared to GD) are not preserved under noise unless it decreases to 0 as the optimization trajectory approaches the solution. See also [24] for further comparisons of noisy GD with or without momentum. Our work refines this picture in the case of sampling noise. Our results in Section 4 suggest that including positive momentum in SGD always improves convergence in the signal-dominated phase, but generally not in the noise-dominated phase (where it may even be beneficial to use a negative momentum).

**Optimization of batch size.** It is known that for SGD with not too large batches, there is approximately linear scalability of learning w.r.t. batch size, in the sense that to reach a given loss value with an increased batch size the number of iterations should be decreased proportionally [30, 41]. This law is naturally no longer valid at very large batch sizes, since in the limit of infinitely large batch size SGD just converges to the non-stochastic GD, so that further increasing batch size when it is already large brings little benefit (the effect of “diminishing returns”). Our theoretical analysis in Section 4 based on large- $t$  loss asymptotics is consistent with linear scalability.

## B Details of the setting

### B.1 Basics

In our problem setting we always consider regression tasks of fitting target function  $y^*(\mathbf{x})$  using linear models  $f(\mathbf{x}, \mathbf{w})$  of the form

$$f(\mathbf{x}, \mathbf{w}) = \langle \mathbf{w}, \psi(\mathbf{x}) \rangle \quad (29)$$

where  $\langle \cdot, \cdot \rangle$  stands for a scalar product and  $\psi(\mathbf{x})$  are some (presumably non-linear) features of inputs  $\mathbf{x}$ . The space  $\mathcal{X}$  containing inputs  $\mathbf{x}$  is not important in our context. Next, the model will be always trained to minimize a quadratic loss function over training dataset  $\mathcal{D}$ :

$$L(\mathbf{w}) = \frac{1}{2} \mathbb{E}_{\mathbf{x} \sim \mathcal{D}} (\langle \mathbf{w}, \psi(\mathbf{x}) \rangle - y^*(\mathbf{x}))^2. \quad (30)$$

Denote by  $B_t$  a set of  $b = |B_t|$  training samples  $\mathbf{x}$  drawn independently and uniformly without replacement from  $\mathcal{D}$ . Then a single step of SGD with learning rate  $\alpha_t$  and momentum parameter  $\beta_t$  takes the form

$$\begin{pmatrix} \mathbf{w}_{t+1} \\ \mathbf{v}_{t+1} \end{pmatrix} = \begin{pmatrix} \mathbf{I} - \alpha_t \mathbf{H}(B_t) & \beta_t \mathbf{I} \\ -\alpha_t \mathbf{H}(B_t) & \beta_t \mathbf{I} \end{pmatrix} \begin{pmatrix} \mathbf{w}_t \\ \mathbf{v}_t \end{pmatrix} + \begin{pmatrix} \alpha_t \mathbf{h}(B_t) \\ \alpha_t \mathbf{h}(B_t) \end{pmatrix} \quad (31)$$

$$\mathbf{H}(B_t) \equiv \frac{1}{b} \sum_{\mathbf{x}_i \in B_t} \psi(\mathbf{x}_i) \otimes \psi(\mathbf{x}_i) \quad (32)$$

$$\mathbf{h}(B_t) \equiv \frac{1}{b} \sum_{\mathbf{x}_i \in B_t} \psi(\mathbf{x}_i) y^*(\mathbf{x}_i) \quad (33)$$

Note that expression (31) of SGD step is equivalent to more compact expression (2) when there exist optimal parameters  $\mathbf{w}^*$  such that  $\langle \mathbf{w}^*, \psi(\mathbf{x}) \rangle = y^*(\mathbf{x})$ . As we have already noticed, existence of optimal parameters with  $\|\mathbf{w}^*\| < \infty$  may not be the case for models relevant to practical problems (e.g. MNIST). Thus we will consider (31) to be the basic form of SGD step in our work. However, formal usage (2) instead of (31) always lead to the same conclusions and therefore we focused on the case  $\|\mathbf{w}^*\| < \infty$  in the main paper. In subsection B.3 we consider formulation of SGD in output space, which allows to treat cases  $\|\mathbf{w}^*\| = \infty$  and  $\|\mathbf{w}^*\| < \infty$  within the same framework.

It is convenient to distinguish several cases of our problem setting different by finite/infinite dimensionality  $d$  of parameters  $\mathbf{w}$ , and finite/infinite size  $|\mathcal{D}| = N$  of the dataset used for training. In our work we take into account all these cases, as each of them is used in either experimental or theoretical part of the paper.

### B.2 Eigendecompositions and other details

**Case 1:**  $d, N < \infty$ . This is the simplest case and we will often repeat the respective paragraph of section 2. First, it is convenient to consider the  $d \times N$  Jacobian matrix  $\Psi$

$$\Psi_{ij} = \frac{1}{\sqrt{N}} \psi_i(\mathbf{x}_j), \quad \mathbf{x}_j \in \mathcal{D} \quad (34)$$

We will assume without loss of generality that  $\Psi$  has a full rank  $r = \min(d, N)$  (the general case reduces to this after a suitable projection). Then by (30) the Hessian of the model is

$$\mathbf{H} = \Psi \Psi^T = \frac{1}{N} \sum_{j=1}^N \psi(\mathbf{x}_j) \psi^T(\mathbf{x}_j). \quad (35)$$

Another important matrix is the kernel  $K(\mathbf{x}, \mathbf{x}') = \psi(\mathbf{x})^T \psi(\mathbf{x}')$  calculated on the training dataset  $\mathcal{D}$

$$\mathbf{K} = \Psi^T \Psi = \frac{1}{N} \left( \sum_{i=1}^d \psi_i(\mathbf{x}_j) \psi_i(\mathbf{x}_{j'}) \right)_{j,j'=1}^N \quad (36)$$

Next, consider the SVD decomposition of Jacobian  $\Psi = \mathbf{U} \Lambda \mathbf{V}$  with  $\mathbf{U} = (\mathbf{u}_k)_{k=1}^d$  being the matrix of left eigenvectors,  $\mathbf{V} = (\phi_k^T)_{k=1}^N$  being the matrix of right eigenvectors, and rectangular  $d \times N$  diagonal matrix with singular values  $\Lambda_{kk} = \sqrt{\lambda_k}$ ,  $k = 1 \dots r$  on the diagonal. The Hessian and kernel matrices are symmetric and have eigendecompositions with shared spectrum of non-zero eigenvalues:  $\lambda_k, \mathbf{u}_k$  for  $\mathbf{H}$  and  $\lambda_k, \mathbf{v}_k$  for  $\mathbf{K}$ .

Now let us proceed to the target function  $y^*(\mathbf{x})$ . As in this paper we focus on the training error (30), we may also restrict ourselves to the target vector  $\mathbf{y}^*$  of target function values at training points:  $y_i^* = \frac{1}{\sqrt{N}} y^*(\mathbf{x}_i)$ ,  $\mathbf{x}_i \in \mathcal{D}$ . The normalization by  $\sqrt{N}$  is done here to allow for direct correspondence with the  $N = \infty$  case. If  $d \leq N$ , we recall our assumption of  $\Psi$  having full rank and therefore the target function is reachable since the equation  $\mathbf{w}^T \Psi = \mathbf{y}^*$  always has a solution. However, if  $d < N$ , there are many possible solutions of  $\mathbf{w}^T \Psi = \mathbf{y}^*$ , and we choose  $\mathbf{w}^*$  to be the one with the same projection on  $\ker \mathbf{H}$  as the initial model parameters  $\mathbf{w}_0$ . Later, this choice will guarantee that during SGD dynamic (31) parameter deviation always lies in the image of the Hessian:  $\Delta \mathbf{w}_t \equiv \mathbf{w}_t - \mathbf{w}^* \in \text{Im } \mathbf{H}$ . Finally, if  $N > d$ , the target may be unreachable:  $\mathbf{y}^* \notin \text{Im } \Psi^T$ . In this case we consider the decomposition of the output space  $\mathbb{R}^N = \text{Im } \mathbf{K} \oplus \ker \mathbf{K}$  and the respective decomposition of target vector  $\mathbf{y}^* = \mathbf{y}_{\parallel}^* + \mathbf{y}_{\perp}^*$ . Then  $\mathbf{y}_{\parallel}^*$  is always reachable  $\mathbf{y}_{\parallel}^* \in \text{Im } \Psi^T$  and in the rest we simply consider reachable part of the target  $\mathbf{y}_{\parallel}^*$  instead of the original target  $\mathbf{y}^*$ .

Apart from general finite regression problems, the case  $d, N < \infty$  described above applies to linearization of practical neural networks (and other parametric models). Specifically, consider a model  $f(\mathbf{w}, \mathbf{x})$  initialized at  $\mathbf{w}_0$  with initial predictions  $f_0(\mathbf{x}) \equiv f(\mathbf{w}_0, \mathbf{x})$ . The training of linearized model  $f(\mathbf{w}, \mathbf{x}) = f_0(\mathbf{x}) + \langle \mathbf{w} - \mathbf{w}_0, \nabla_{\mathbf{w}} f(\mathbf{w}_0, \mathbf{x}) \rangle$  can be mapped to out basic problem setting (29) with replacements  $\psi(\mathbf{x}) \leftarrow \nabla_{\mathbf{w}} f(\mathbf{w}_0, \mathbf{x})$ ,  $\mathbf{w} \leftarrow \mathbf{w} - \mathbf{w}_0$ ,  $y^*(\mathbf{x}) \leftarrow y^*(\mathbf{x}) - f_0(\mathbf{x})$ .

**Case 2:**  $d = \infty, N < \infty$ . In this case we assume that model parameters  $\mathbf{w}$  and features  $\psi(\mathbf{x})$  belong to a Hilbert space  $\mathcal{H}$ , and  $\langle \cdot, \cdot \rangle$  denotes the scalar product in  $\mathcal{H}$ . For the Hessian we have

$$\mathbf{H} = \frac{1}{N} \sum_{j=1}^N \psi(\mathbf{x}_j) \otimes \psi(\mathbf{x}_j), \quad \mathbf{x}_j \in \mathcal{D} \quad (37)$$

We assume that the features  $\psi(\mathbf{x}_j)$ ,  $\mathbf{x}_j \in \mathcal{D}$  are linearly independent (as is usually the case in practice), then  $\dim \text{Im } \mathbf{H} = N < \infty$ . As SGD updates occur in  $\text{Im } \mathbf{H}$ , we again use space decomposition  $\mathcal{H} = \text{Im } \mathbf{H} \oplus \ker \mathbf{H}$  and respective decomposition of parameters  $\mathbf{w} = \mathbf{w}_{\parallel} + \mathbf{w}_{\perp}$  and features  $\psi(\mathbf{x}) = \psi(\mathbf{x})_{\parallel} + \psi(\mathbf{x})_{\perp}$ . As  $\psi(\mathbf{x}_j)_{\perp} = 0$ ,  $\mathbf{x}_j \in \mathcal{D}$  and  $\mathbf{w}_{\perp}$  do not affect the loss (30) we can restrict ourselves to  $\text{Im } \mathbf{H}$  which bring us to finite dimensional case  $d = N < \infty$  fully described above.

The case  $d = \infty, N < \infty$  is primarily used for kernel regression problems defined by a kernel function  $K(\mathbf{x}, \mathbf{x}')$  which can be, for example, one of the "classical" kernels (e.g. Gaussian) or Neural Tangent Kernel (NTK) of some infinitely wide neural network. In this case  $\mathcal{H}$  is a reproducing kernel Hilbert space (RKHS) of the kernel  $K(\mathbf{x}, \mathbf{x}')$ , and features  $\psi(\mathbf{x})$  are the respective mappings  $\psi : \mathcal{X} \rightarrow \mathcal{H}$  with the property  $K(\mathbf{x}, \mathbf{x}') = \langle \psi(\mathbf{x}), \psi(\mathbf{x}') \rangle$ .

**Case 3:**  $d, N = \infty$ . We are particularly interested in the case  $d = N = \infty$  because in practice  $N$  is quite large and, as previously discussed, the eigenvalues  $\lambda_k$  and target expansion coefficients often are distributed according to asymptotic power laws, which all suggests working in an infinite-dimensional setting. A standard approach to rigorously accommodate  $N = \infty$ , which we sketch now, is based on Mercer's theorem.

We describe the infinite ( $N = \infty$ ) training dataset by a probability measure  $\mu(\mathbf{x})$  so that the loss takes the form

$$L(\mathbf{w}) = \frac{1}{2} \int (\langle \mathbf{w}, \psi(\mathbf{x}) \rangle - y^*(\mathbf{x}))^2 d\mu(\mathbf{x}) = \frac{1}{2} \|\langle \mathbf{w}, \psi(\mathbf{x}) \rangle - y^*(\mathbf{x})\|_{\mathcal{F}}^2, \quad (38)$$



assuming that  $\|y^*(\mathbf{x})\|_{\mathcal{F}}^2 < \infty$  for the loss to be well defined. Here in addition to the Hilbert space of parameters  $\mathcal{H} \ni \mathbf{w}$  we introduced the Hilbert space  $\mathcal{F}$  of square integrable functions  $f(\mathbf{x}) : \|f\|_{\mathcal{F}}^2 \equiv \int f(\mathbf{x})^2 d\mu(\mathbf{x}) < \infty$ . The Hessian  $\mathbf{H}$ , and the counterparts of the kernel and feature matrices  $\mathbf{K}$  (36) and  $\Psi$  (34) are now operators

$$\mathbf{H} : \mathcal{H} \rightarrow \mathcal{H}, \quad \mathbf{H} = \int \psi(\mathbf{x}) \otimes \psi(\mathbf{x}) d\mu(\mathbf{x}) \quad (39)$$

$$\mathbf{K} : \mathcal{F} \rightarrow \mathcal{F}, \quad \mathbf{K}g(x) = \int K(\mathbf{x}, \mathbf{x}') g(\mathbf{x}') d\mu(\mathbf{x}') \quad (40)$$

$$\Psi : \mathcal{F} \rightarrow \mathcal{H}, \quad \Psi g(x) = \int \psi(\mathbf{x}') g(\mathbf{x}') d\mu(\mathbf{x}') \quad (41)$$

Again, due to our interest in convergence of the loss (30) during SGD (31), we project parameters  $\mathbf{w}$  to  $\mathcal{H} \ominus \ker \mathbf{H}$  and target function  $y^*(\mathbf{x})$  to  $\mathcal{F} \ominus \ker \mathbf{K}$ . After this projection the target is reachable in the sense that  $y^*(\mathbf{x}) \in \mathcal{F} \ominus \ker \mathbf{K} = \overline{\text{Im } \Psi^\dagger}$ . In particular, this means that an optimum such that  $\|\langle \mathbf{w}^*, \psi(\mathbf{x}) \rangle - y^*(\mathbf{x})\| = 0$  may not exist, but there is always a sequence  $\mathbf{w}_n$  such that  $\lim_{n \rightarrow \infty} \|\langle \mathbf{w}_n, \psi(\mathbf{x}) \rangle - y^*(\mathbf{x})\| = 0$

Now we proceed to eigendecompositions of  $\mathbf{H}$  and  $\mathbf{K}$ . According to the Mercer's theorem, the restriction of the operator  $\mathbf{K}$  given by (40) to  $\mathcal{F} \ominus \ker \mathbf{K}$  admits an eigendecomposition of the form

$$\mathbf{K}g(\mathbf{x}) = \sum_{k=1}^{\infty} \lambda_k \phi_k(\mathbf{x}) \int \phi_k(\mathbf{x}') g(\mathbf{x}') d\mu(\mathbf{x}') \quad (42)$$

with  $\lambda_k > 0$ ,  $\int \phi_k(\mathbf{x}) \phi_l(\mathbf{x}) d\mu(\mathbf{x}) = \delta_{kl}$ , and  $\{\phi_k(\mathbf{x})\}$  being a complete basis in  $\mathcal{F} \ominus \ker \mathbf{K}$ . The latter allows to decompose features as

$$\psi(\mathbf{x}) = \sum_k \rho_k \mathbf{u}_k \phi_k(\mathbf{x}) \quad (43)$$

with  $\|\mathbf{u}_k\|^2 = 1$ . Substituting (43) into (40) gives  $\langle \mathbf{u}_k, \mathbf{u}_l \rangle = \delta_{kl}$  and  $\rho_k^2 = \lambda_k$ . Substituting then (43) into (39) gives

$$\mathbf{H} = \sum_{k=1}^{\infty} \lambda_k \mathbf{u}_k \otimes \mathbf{u}_k, \quad (44)$$

which also makes  $\{\mathbf{u}_k\}$  an orthonormal basis in  $\mathcal{H} \ominus \ker \mathbf{H}$ .

Under mild regularity assumptions, one can show [26] that the eigenvalues  $\lambda_k$  converge to 0, and we will assume this in the sequel. Note that if  $\lambda_k \rightarrow 0$ , then the range of the operator  $\Psi^\dagger$  is not closed so that, exactly as pointed out above, for some  $y^*(\mathbf{x}) \in \mathcal{F} \ominus \ker \mathbf{K}$  there are no exact finite-norm minimizers  $\mathbf{w}^* \in \mathcal{H}$  satisfying  $\langle \mathbf{w}^*, \psi(\mathbf{x}) \rangle = y^*(\mathbf{x})$  for  $\mu$ -almost all  $\mathbf{x}$ .

### B.3 Output and parameter spaces

Recall that we only assume  $\int y^*(\mathbf{x})^2 d\mu(\mathbf{x}) < \infty$  but do not guarantee existence of the optimum  $\mathbf{w}^*$  in the case  $N = d = \infty$ . This means that considering SGD dynamics directly in the space of model outputs  $f(\mathbf{x}) = \langle \mathbf{w}, \psi(\mathbf{x}) \rangle$  may be advantageous when  $\mathbf{w}^*$  is not available. Moreover, it will allow to completely bypass construction of parameter space when original problem is formulated in terms of kernel  $K(\mathbf{x}, \mathbf{x}')$  (e.g. for an infinitely wide neural network in the NTK regime). First, let us rewrite SGD recursion in the output space by taking the scalar product of (31) with  $\psi(\mathbf{x})$ :

$$\begin{pmatrix} f_{t+1}(\mathbf{x}) \\ v_{t+1}(\mathbf{x}) \end{pmatrix} = \begin{pmatrix} \mathbf{I} - \alpha_t \mathbf{K}(B_t) & \beta_t \mathbf{I} \\ -\alpha_t \mathbf{K}(B_t) & \beta_t \mathbf{I} \end{pmatrix} \begin{pmatrix} f_t(\mathbf{x}) \\ v_t(\mathbf{x}) \end{pmatrix} + \begin{pmatrix} \alpha_t \mathbf{K}(B_t) y^*(\mathbf{x}) \\ \alpha_t \mathbf{K}(B_t) y^*(\mathbf{x}) \end{pmatrix} \quad (45)$$

$$\mathbf{K}(B_t)g(\mathbf{x}) = \frac{1}{b} \sum_{\mathbf{x}_i \in B_t} K(\mathbf{x}, \mathbf{x}_i) g(\mathbf{x}_i) \quad (46)$$

Here  $v_t(\mathbf{x}) = \langle \mathbf{v}_t, \psi(\mathbf{x}) \rangle = f_t(\mathbf{x}) - f_{t+1}(\mathbf{x})$ . Considering the approximation error  $\Delta f(\mathbf{x}) \equiv f(\mathbf{x}) - y^*(\mathbf{x})$  we get

$$\begin{pmatrix} \Delta f_{t+1}(\mathbf{x}) \\ v_{t+1}(\mathbf{x}) \end{pmatrix} = \begin{pmatrix} \mathbf{I} - \alpha_t \mathbf{K}(B_t) & \beta_t \mathbf{I} \\ -\alpha_t \mathbf{K}(B_t) & \beta_t \mathbf{I} \end{pmatrix} \begin{pmatrix} \Delta f_t(\mathbf{x}) \\ v_t(\mathbf{x}) \end{pmatrix} \quad (47)$$

As (45) is equivalent to (31), we also get that (47) is equivalent to (2) when  $\mathbf{w}^*$  is available. Thus (47) can be considered as the most general and convenient form of writing an SGD iteration.

Similarly to second moments (3) defined for parameter space, we define second moments in the output space:

$$\begin{aligned} C^{\text{out}}(\mathbf{x}, \mathbf{x}') &\equiv \mathbb{E}[\Delta f(\mathbf{x}) \Delta f(\mathbf{x}')] \\ J^{\text{out}}(\mathbf{x}, \mathbf{x}') &\equiv \mathbb{E}[\Delta f(\mathbf{x}) v(\mathbf{x}')] \\ V^{\text{out}}(\mathbf{x}, \mathbf{x}') &\equiv \mathbb{E}[v(\mathbf{x}) v(\mathbf{x}')] \\ \Sigma^{\text{out}}(\mathbf{x}, \mathbf{x}') &\equiv \begin{pmatrix} C^{\text{out}}(\mathbf{x}, \mathbf{x}') & J^{\text{out}}(\mathbf{x}, \mathbf{x}') \\ J^{\text{out}}(\mathbf{x}', \mathbf{x}) & V^{\text{out}}(\mathbf{x}, \mathbf{x}') \end{pmatrix}, \end{aligned} \quad (48)$$

where the superscript  $\text{out}$  indicates the output space (to avoid confusion with the respective moment counterparts defined in the parameter space). The same moments can be written in the eigenbasis  $\{\phi(\mathbf{x})\}$  of the operator  $\mathbf{K}$  according to the rule

$$G_{kl}^{\text{out}} = \int \phi_k(\mathbf{x}) G^{\text{out}}(\mathbf{x}, \mathbf{x}') \phi_l(\mathbf{x}) d\mu(\mathbf{x}), \quad (49)$$

where  $G$  stands for either  $C, F$  or  $V$ . When  $\mathbf{w}^*$  is available, the moments  $C_{kl}^{\text{out}}$  in the output space are related to the moments  $C_{kl}$  in the parameter space simply by

$$C_{kl}^{\text{out}} = \sqrt{\lambda_k \lambda_l} C_{kl}. \quad (50)$$

In particular,

$$C_{kk}^{\text{out}} = \lambda_k C_{kk} \quad (51)$$

and

$$\sum_k \lambda_k C_{kk} = \sum_k C_{kk}^{\text{out}} = \mathbb{E}[\|\Delta f\|^2] < \infty. \quad (52)$$

Even when  $\mathbf{w}^*$  is not available we can still define  $C_{kl}$  by Eq. (50), but in this case  $\sum_k C_{kk} = \infty$ .

## C Dynamics of second moments

### C.1 Derivation of second moments dynamic equation

The purpose of this section is to prove proposition 1. However, as discussed in section B.3, the description in terms of moments in output space (48) is more widely applicable than description in terms of parameter moments (3). Thus we first prove an analogue of proposition 1 for output space moments. For convinience, let us denote the moments (48) as  $\mathbf{C}^{\text{out}}, \mathbf{J}^{\text{out}}, \mathbf{V}^{\text{out}} \in \mathcal{F} \otimes \mathcal{F}$ .

**Proposition 4.** Consider SGD (47) with learning rates  $\alpha_t$ , momentum  $\beta_t$ , batch size  $b$  and random uniform choice of the batch  $B_t$ . Then the update of second moments (48) is

$$\begin{aligned} \begin{pmatrix} \mathbf{C}_{t+1}^{\text{out}} & \mathbf{J}_{t+1}^{\text{out}} \\ (\mathbf{J}_{t+1}^{\text{out}})^\dagger & \mathbf{V}_{t+1}^{\text{out}} \end{pmatrix} &= \begin{pmatrix} \mathbf{I} - \alpha_t \mathbf{K} & \beta_t \mathbf{I} \\ -\alpha_t \mathbf{K} & \beta_t \mathbf{I} \end{pmatrix} \begin{pmatrix} \mathbf{C}_t^{\text{out}} & \mathbf{J}_t^{\text{out}} \\ (\mathbf{J}_t^{\text{out}})^\dagger & \mathbf{V}_t^{\text{out}} \end{pmatrix} \begin{pmatrix} \mathbf{I} - \alpha_t \mathbf{K} & \beta_t \mathbf{I} \\ -\alpha_t \mathbf{K} & \beta_t \mathbf{I} \end{pmatrix}^T \\ &\quad + \gamma \alpha_t^2 \begin{pmatrix} \hat{D}^{\text{out}} \mathbf{C}_t^{\text{out}} & \hat{D}^{\text{out}} \mathbf{C}_t^{\text{out}} \\ \hat{D}^{\text{out}} \mathbf{C}_t^{\text{out}} & \hat{D}^{\text{out}} \mathbf{C}_t^{\text{out}} \end{pmatrix} \end{aligned} \quad (53)$$

The second term represents sampling noise and is given by

1) for finite dataset  $\mathcal{D} = \{\mathbf{x}_i\}_{i=1}^N$ :

$$\hat{D}^{\text{out}} \mathbf{C}^{\text{out}}(\mathbf{x}, \mathbf{x}') = \frac{1}{N} \sum_{\mathbf{x}_i \in \mathcal{D}} K(\mathbf{x}, \mathbf{x}_i) C^{\text{out}}(\mathbf{x}_i, \mathbf{x}_i) K(\mathbf{x}_i, \mathbf{x}') - \mathbf{K} \mathbf{C}^{\text{out}} \mathbf{K}(\mathbf{x}, \mathbf{x}'), \quad (54)$$

and the amplitude  $\gamma = \frac{N-b}{(N-1)b}$ ;

2) for infinite dataset  $\mathcal{D}$  with density  $d\mu(\mathbf{x})$ :

$$\hat{D}^{\text{out}} \mathbf{C}^{\text{out}}(\mathbf{x}, \mathbf{x}') = \int K(\mathbf{x}, \mathbf{x}'') C^{\text{out}}(\mathbf{x}'', \mathbf{x}'') K(\mathbf{x}'', \mathbf{x}') d\mu(\mathbf{x}'') - \mathbf{K} \mathbf{C}^{\text{out}} \mathbf{K}(\mathbf{x}, \mathbf{x}'), \quad (55)$$

and the amplitude  $\gamma = \frac{1}{b}$ .

*Proof.* First, we take expression of single SGD (47) and use it to express  $\Sigma_{t+1}^{\text{out}}$  through  $\Sigma_t^{\text{out}}$ .

$$\begin{aligned}
\Sigma_{t+1}^{\text{out}}(\mathbf{x}, \mathbf{x}') &= \mathbb{E} \left[ \begin{pmatrix} \Delta f_{t+1}(\mathbf{x}) \Delta f_{t+1}(\mathbf{x}') & \Delta f_{t+1}(\mathbf{x}) v_{t+1}(\mathbf{x}') \\ v_{t+1}(\mathbf{x}) \Delta f_{t+1}(\mathbf{x}') & v_{t+1}(\mathbf{x}) v_{t+1}(\mathbf{x}') \end{pmatrix} \right] \\
&= \mathbb{E} \left[ \begin{pmatrix} \mathbf{I} - \alpha_t \mathbf{K}(B_t) & \beta_t \mathbf{I} \\ -\alpha_t \mathbf{K}(B_t) & \beta_t \mathbf{I} \end{pmatrix} \begin{pmatrix} \Delta f_t(\mathbf{x}) \\ v_t(\mathbf{x}) \end{pmatrix} \begin{pmatrix} \Delta f_t(\mathbf{x}') & v_t(\mathbf{x}') \end{pmatrix} \begin{pmatrix} \mathbf{I} - \alpha_t \mathbf{K}(B_t) & \beta_t \mathbf{I} \\ -\alpha_t \mathbf{K}(B_t) & \beta_t \mathbf{I} \end{pmatrix}^T \right] \\
&\stackrel{(1)}{=} \mathbb{E} \left[ \begin{pmatrix} \mathbf{I} - \alpha_t \mathbf{K}(B_t) & \beta_t \mathbf{I} \\ -\alpha_t \mathbf{K}(B_t) & \beta_t \mathbf{I} \end{pmatrix} \begin{pmatrix} \mathbf{C}_t^{\text{out}} & \mathbf{J}_t^{\text{out}} \\ (\mathbf{J}_t^{\text{out}})^\dagger & \mathbf{V}_t^{\text{out}} \end{pmatrix} \begin{pmatrix} \mathbf{I} - \alpha_t \mathbf{K}(B_t) & \beta_t \mathbf{I} \\ -\alpha_t \mathbf{K}(B_t) & \beta_t \mathbf{I} \end{pmatrix}^T \right] \\
&\stackrel{(2)}{=} \begin{pmatrix} \mathbf{I} - \alpha_t \mathbf{K} & \beta_t \mathbf{I} \\ -\alpha_t \mathbf{K} & \beta_t \mathbf{I} \end{pmatrix} \begin{pmatrix} \mathbf{C}_t^{\text{out}} & \mathbf{J}_t^{\text{out}} \\ (\mathbf{J}_t^{\text{out}})^\dagger & \mathbf{V}_t^{\text{out}} \end{pmatrix} \begin{pmatrix} \mathbf{I} - \alpha_t \mathbf{K} & \beta_t \mathbf{I} \\ -\alpha_t \mathbf{K} & \beta_t \mathbf{I} \end{pmatrix}^T \\
&\quad + \begin{pmatrix} \mathbb{E} [\delta \mathbf{K}(B_t) \mathbf{C}_t^{\text{out}} \delta \mathbf{K}(B_t)] & \mathbb{E} [\delta \mathbf{K}(B_t) \mathbf{C}_t^{\text{out}} \delta \mathbf{K}(B_t)] \\ \mathbb{E} [\delta \mathbf{K}(B_t) \mathbf{C}_t^{\text{out}} \delta \mathbf{K}(B_t)] & \mathbb{E} [\delta \mathbf{K}(B_t) \mathbf{C}_t^{\text{out}} \delta \mathbf{K}(B_t)] \end{pmatrix}
\end{aligned} \tag{56}$$

Here in (1) we used that  $\Delta f_t, v_t$  are independent from  $B_t$  and therefore the average factorizes into product of averages. In (2) we introduced notation  $\delta \mathbf{K}(B_t) = \mathbf{K}(B_t) - \mathbf{K}$  and used that  $\mathbb{E}[\delta \mathbf{K}(B_t)] = 0$ .

Now we proceed to the calculation of the average from the last line in (56):

$$\gamma \widehat{D}^{\text{out}} \mathbf{C}^{\text{out}} \equiv \mathbb{E} [\delta \mathbf{K}(B_t) \mathbf{C}^{\text{out}} \delta \mathbf{K}(B_t)] \tag{57}$$

1) Finite  $\mathcal{D} = \{\mathbf{x}_i\}_{i=1}^N$ .

Denoting for convenience function values calculated at  $\mathbf{x}_i, \mathbf{x}_j$  with subscripts  $ij$ , we get

$$\begin{aligned}
\gamma (\widehat{D}^{\text{out}} \mathbf{C}^{\text{out}})_{ij} &= \mathbb{E} \left[ \left( \delta \mathbf{K}(B) \mathbf{C}^{\text{out}} \delta \mathbf{K}(B) \right)_{ij} \right] \\
&= \mathbb{E} \left[ \left( \frac{1}{b} \sum_{i' \in B} - \frac{1}{N} \sum_{i'} \right) \left( \frac{1}{b} \sum_{j' \in B} - \frac{1}{N} \sum_{j'} \right) K_{ii'} K_{jj'} C_{i'j'}^{\text{out}} \right] \\
&= \mathbb{E} \left[ \left( \frac{1}{b^2} \sum_{i', j' \in B} - \frac{1}{N^2} \sum_{i', j'} \right) K_{ii'} K_{jj'} C_{i'j'}^{\text{out}} \right] \\
&\stackrel{(1)}{=} \left( \left( \frac{1}{b^2} \frac{b}{N} - \frac{1}{N^2} \right) \sum_{i'=j'} + \left( \frac{1}{|B|^2} \frac{b(b-1)}{N(N-1)} - \frac{1}{N^2} \right) \sum_{i' \neq j'} \right) K_{ii'} K_{jj'} C_{i'j'}^{\text{out}} \\
&= \left( \frac{N-b}{b} \sum_{i'=j'} - \frac{N-b}{b(N-1)} \sum_{i' \neq j'} \right) \frac{1}{N^2} K_{ii'} K_{jj'} C_{i'j'}^{\text{out}} \\
&= \frac{N-b}{(N-1)b} \sum_{i'j'} (N \delta_{i'j'} - 1) \frac{1}{N^2} K_{ii'} K_{jj'} C_{i'j'}^{\text{out}}
\end{aligned} \tag{58}$$

Here unspecified sums run over dataset  $\mathcal{D}$ . In (1) we used that the fraction of batches  $B$  which contain two indices  $i' \neq j'$  is  $\binom{N-2}{|B|-2} / \binom{N}{|B|} = \frac{|B|(|B|-1)}{N(N-1)}$  and the fraction of batches containing index  $j'$  is  $\binom{N-1}{|B|-1} / \binom{N}{|B|} = \frac{|B|}{N}$ . Taking  $\gamma = \frac{N-b}{(N-1)b}$  we get (54)

2) Infinite  $\mathcal{D}$  with density  $d\mu(\mathbf{x})$ . Proceeding similarly to (58) we get

$$\begin{aligned}\widehat{\mathbf{D}}^{\text{out}} \mathbf{C}^{\text{out}}(\mathbf{x}, \mathbf{x}') &= \mathbb{E} [\mathbf{K}(B) \mathbf{C}^{\text{out}} \mathbf{K}(B)](\mathbf{x}, \mathbf{x}') - \mathbf{K} \mathbf{C}^{\text{out}} \mathbf{K}(\mathbf{x}, \mathbf{x}') \\ &= \frac{b}{b^2} \int K(\mathbf{x}, \mathbf{x}'') \mathbf{C}^{\text{out}}(\mathbf{x}'', \mathbf{x}') K(\mathbf{x}'', \mathbf{x}') d\mu(\mathbf{x}'') \\ &\quad + \frac{b(b-1)}{b^2} \mathbf{K} \mathbf{C}^{\text{out}} \mathbf{K}(\mathbf{x}, \mathbf{x}') - \mathbf{K} \mathbf{C}^{\text{out}} \mathbf{K}(\mathbf{x}, \mathbf{x}') \\ &= \frac{1}{b} \left( \int K(\mathbf{x}, \mathbf{x}'') \mathbf{C}^{\text{out}}(\mathbf{x}'', \mathbf{x}') K(\mathbf{x}'', \mathbf{x}') d\mu(\mathbf{x}'') - \mathbf{K} \mathbf{C}^{\text{out}} \mathbf{K}(\mathbf{x}, \mathbf{x}') \right)\end{aligned}\tag{59}$$

which gives (55) after setting  $\gamma = \frac{1}{b}$ .  $\square$

Let us write second moments dynamics for both parameter space (4) and output space (53) in eigenbases  $\{\mathbf{u}_k\}$  and  $\{\phi_k(\mathbf{x})\}$  using decompositions (43) and (42). For parameter space we get

$$\begin{aligned}\begin{pmatrix} C_{kl,t+1} & J_{kl,t+1} \\ J_{lk,t+1} & V_{kl,t+1} \end{pmatrix} &= \begin{pmatrix} 1 - \alpha_t \lambda_k & \beta_t \\ -\alpha_t \lambda_k & \beta_t \end{pmatrix} \begin{pmatrix} C_{kl,t} & J_{kl,t} \\ J_{lk,t} & V_{kl,t} \end{pmatrix} \begin{pmatrix} 1 - \alpha_t \lambda_l & \beta_t \\ -\alpha_t \lambda_l & \beta_t \end{pmatrix}^T \\ &\quad + \gamma \alpha_t^2 \sqrt{\lambda_k \lambda_l} \left( \sum_{k'l'} \sqrt{\lambda_{k'} \lambda_{l'}} C_{k'l',t} \int \phi_k(\mathbf{x}) \phi_l(\mathbf{x}) \phi_{k'}(\mathbf{x}) \phi_{l'}(\mathbf{x}) d\mu(\mathbf{x}) - C_{kl,t} \right) \begin{pmatrix} 1 & 1 \\ 1 & 1 \end{pmatrix}\end{aligned}\tag{60}$$

And for output space

$$\begin{aligned}\begin{pmatrix} C_{kl,t+1}^{\text{out}} & J_{kl,t+1}^{\text{out}} \\ J_{lk,t+1}^{\text{out}} & V_{kl,t+1}^{\text{out}} \end{pmatrix} &= \begin{pmatrix} 1 - \alpha_t \lambda_k & \beta_t \\ -\alpha_t \lambda_k & \beta_t \end{pmatrix} \begin{pmatrix} C_{kl,t}^{\text{out}} & J_{kl,t}^{\text{out}} \\ J_{lk,t}^{\text{out}} & V_{kl,t}^{\text{out}} \end{pmatrix} \begin{pmatrix} 1 - \alpha_t \lambda_l & \beta_t \\ -\alpha_t \lambda_l & \beta_t \end{pmatrix}^T \\ &\quad + \gamma \alpha_t^2 \lambda_k \lambda_l \left( \sum_{k'l'} C_{k'l',t}^{\text{out}} \int \phi_k(\mathbf{x}) \phi_l(\mathbf{x}) \phi_{k'}(\mathbf{x}) \phi_{l'}(\mathbf{x}) d\mu(\mathbf{x}) - C_{kl,t}^{\text{out}} \right) \begin{pmatrix} 1 & 1 \\ 1 & 1 \end{pmatrix}\end{aligned}\tag{61}$$

Now we are ready to prove proposition 1

**Proposition 1.** Consider SGD (1) with learning rates  $\alpha_t$ , momentum  $\beta_t$ , batch size  $b$  and random uniform choice of the batch  $B_t$ . Then the update of second moments (3) is

$$\begin{pmatrix} \mathbf{C}_{t+1} & \mathbf{J}_{t+1} \\ \mathbf{J}_{t+1}^\dagger & \mathbf{V}_{t+1} \end{pmatrix} = \begin{pmatrix} \mathbf{I} - \alpha_t \mathbf{H} & \beta_t \mathbf{I} \\ -\alpha_t \mathbf{H} & \beta_t \mathbf{I} \end{pmatrix} \begin{pmatrix} \mathbf{C}_t & \mathbf{J}_t \\ \mathbf{J}_t^\dagger & \mathbf{V}_t \end{pmatrix} \begin{pmatrix} \mathbf{I} - \alpha_t \mathbf{H} & \beta_t \mathbf{I} \\ -\alpha_t \mathbf{H} & \beta_t \mathbf{I} \end{pmatrix}^T + \gamma \alpha_t^2 \begin{pmatrix} \widehat{\mathbf{D}} \mathbf{C}_t & \widehat{\mathbf{D}} \mathbf{C}_t \\ \widehat{\mathbf{D}} \mathbf{C}_t & \widehat{\mathbf{D}} \mathbf{C}_t \end{pmatrix}\tag{4}$$

The second term represents sampling noise and is given by

$$\widehat{\mathbf{D}} \mathbf{C} = \frac{1}{N} \sum_{i=1}^N \langle \psi(\mathbf{x}_i), \mathbf{C} \psi(\mathbf{x}_i) \rangle \psi(\mathbf{x}_i) \otimes \psi(\mathbf{x}_i) - \mathbf{H} \mathbf{C} \mathbf{H}\tag{5}$$

with the amplitude  $\gamma = \frac{N-b}{(N-1)b}$  simplifying to  $\gamma = \frac{1}{b}$  in the large dataset limit  $N \rightarrow \infty$ .

*Proof.* Note that in the eigenbasis  $\{\phi_k(\mathbf{x})\}$  of  $\mathbf{K}$  and eigenbasis  $\{\mathbf{u}_k\}$  of  $\mathbf{H}$  output and parameter second moments are connected as

$$\sqrt{\lambda_k \lambda_l} \Sigma_{kl} = \Sigma_{kl}^{\text{out}}\tag{62}$$

Using this connection rule we see that parameter dynamics (60) in eigenbasis of  $\mathbf{H}$  is equivalent to output space second moments dynamics (61) in the eigenbasis of  $\mathbf{K}$ . Finally, (61) is equivalent to (53) proved in 4.  $\square$

For completeness, let us also write a formula of SD approximation in output space:

$$\begin{aligned}\begin{pmatrix} C_{kk,n+1}^{\text{out}} & J_{kk,n+1}^{\text{out}} \\ J_{kk,n+1}^{\text{out}} & V_{kk,n+1}^{\text{out}} \end{pmatrix} &= \begin{pmatrix} 1 - \alpha_t \lambda_k & \beta_t \\ -\alpha_t \lambda_k & \beta_t \end{pmatrix} \begin{pmatrix} C_{kk,t}^{\text{out}} & J_{kk,t}^{\text{out}} \\ J_{kk,t}^{\text{out}} & V_{kk,t}^{\text{out}} \end{pmatrix} \begin{pmatrix} 1 - \alpha_t \lambda_k & \beta_t \\ -\alpha_t \lambda_k & \beta_t \end{pmatrix}^T \\ &\quad + \gamma (\alpha_t \lambda_k)^2 \left( \sum_l C_{ll,t}^{\text{out}} - \tau C_{kk,t} \right) \begin{pmatrix} 1 & 1 \\ 1 & 1 \end{pmatrix}.\end{aligned}\tag{63}$$

## C.2 Translation invariant models

The purpose of this section is to prove Proposition 2.

**Proposition 2.** *Consider a translation invariant problem with dataset forming a regular grid  $\mathcal{D} = \{\mathbf{x}_i = (\frac{2\pi i_1}{N_1}, \dots, \frac{2\pi i_d}{N_d})\}$ ,  $\mathbf{i} \in (\mathbb{Z}/N_1\mathbb{Z}) \times \dots \times (\mathbb{Z}/N_d\mathbb{Z})$  on a  $d$ -dimensional torus  $\mathbb{S}^d$  and with translation invariant kernel  $K(\mathbf{x}, \mathbf{x}') = K(\mathbf{x} - \mathbf{x}')$ . Then  $(\widehat{D}\mathbf{C})_{kk} = (\widehat{D}_{SD}(\tau = 1)\mathbf{C})_{kk}$ .*

*Proof.* Denote the grid-indexing set  $(\mathbb{Z}/N_1\mathbb{Z}) \times \dots \times (\mathbb{Z}/N_d\mathbb{Z})$  by  $\mathbb{Z}/\mathbf{N}\mathbb{Z}$ . Thanks to translation invariance of the data set and kernel, the eigenvectors  $\mathbf{u}_k$  of  $\mathbf{H}$  have an explicit representation in the  $\mathbf{x}$ -domain in terms of Fourier modes. Specifically, let  $\mathbf{K}$  be the  $N \times N$  kernel matrix with matrix elements

$$K_{ij} = K_{i-j} = K_{j-i} = \frac{1}{N} \langle \psi(\mathbf{x}_i), \psi(\mathbf{x}_j) \rangle, \quad \mathbf{i}, \mathbf{j} \in \mathbb{Z}/\mathbf{N}\mathbb{Z}. \quad (64)$$

Consider the functions  $\phi_{\mathbf{k}} : \mathcal{D} \rightarrow \mathbb{C}$  given by

$$\phi_{\mathbf{k}}(\mathbf{x}_i) = N^{-1/2} e^{\sqrt{-1}\mathbf{k} \cdot \mathbf{x}_i} \equiv \phi_{\mathbf{k}\mathbf{i}}, \quad \mathbf{k} \in \mathbb{Z}/\mathbf{N}\mathbb{Z}. \quad (65)$$

These functions form an orthonormal basis in  $\mathbb{C}^{\mathcal{D}}$  and diagonalize the matrix  $\mathbf{K}$ :

$$K_{ij} = \sum_{\mathbf{k} \in \mathbb{Z}/\mathbf{N}\mathbb{Z}} \lambda_{\mathbf{k}} \phi_{\mathbf{k}\mathbf{i}} \bar{\phi}_{\mathbf{k}\mathbf{j}} \quad (66)$$

with

$$\lambda_{\mathbf{k}} = \sum_{\mathbf{i} \in \mathbb{Z}/\mathbf{N}\mathbb{Z}} K_{\mathbf{i}} \phi_{\mathbf{k}\mathbf{i}}. \quad (67)$$

Operator  $\mathbf{H}$  is unitarily equivalent to  $\mathbf{K}$  up to its nullspace. Assuming for convenience that the Hilbert space of  $\mathbf{H}$  is complexified, the respective normalized eigenvectors  $\mathbf{u}_{\mathbf{k}}$  of  $\mathbf{H}$  can be written as

$$\mathbf{u}_{\mathbf{k}} = (N\lambda_{\mathbf{k}})^{-1/2} \sum_{\mathbf{i} \in \mathbb{Z}/\mathbf{N}\mathbb{Z}} \psi(\mathbf{x}_i) \phi_{\mathbf{k}\mathbf{i}}, \quad \mathbf{H}\mathbf{u}_{\mathbf{k}} = \lambda_{\mathbf{k}} \mathbf{u}_{\mathbf{k}}. \quad (68)$$

Assume for the moment that the problem is nondegenerate in the sense that all  $\lambda_{\mathbf{k}} > 0$  so that all the vectors  $\mathbf{u}_{\mathbf{k}}$  are well-defined. It follows in particular that the indices  $k$  of the eigenvalues  $\lambda_k$  can be identified with  $\mathbf{k} \in \mathbb{Z}/\mathbf{N}\mathbb{Z}$ . By inverting relation (68),

$$\psi(\mathbf{x}_i) = \sum_{\mathbf{k} \in \mathbb{Z}/\mathbf{N}\mathbb{Z}} (N\lambda_{\mathbf{k}})^{1/2} \mathbf{u}_{\mathbf{k}} \bar{\phi}_{\mathbf{k}\mathbf{i}}. \quad (69)$$

We can then write, using Eq. (5) and Eqs. (65), (69),

$$(\widehat{D}\mathbf{C})_{\mathbf{k}\mathbf{k}} = \left( \frac{1}{N} \sum_{i=1}^N \langle \psi(\mathbf{x}_i), \mathbf{C}\psi(\mathbf{x}_i) \rangle \psi(\mathbf{x}_i) \otimes \psi(\mathbf{x}_i) - \mathbf{H}\mathbf{C}\mathbf{H} \right)_{\mathbf{k}\mathbf{k}} \quad (70)$$

$$= N \sum_{\mathbf{i}} \lambda_{\mathbf{k}} \phi_{\mathbf{k}\mathbf{i}} \bar{\phi}_{\mathbf{k}\mathbf{i}} \sum_{\mathbf{k}', \mathbf{l}'} \lambda_{\mathbf{k}'}^{1/2} C_{\mathbf{k}'\mathbf{l}'} \lambda_{\mathbf{l}'}^{1/2} \bar{\phi}_{\mathbf{k}'\mathbf{i}} \phi_{\mathbf{l}'\mathbf{i}} - \lambda_{\mathbf{k}}^2 C_{\mathbf{k}\mathbf{k}} \quad (71)$$

$$= \lambda_{\mathbf{k}} \sum_{\mathbf{k}', \mathbf{l}'} \lambda_{\mathbf{k}'}^{1/2} \lambda_{\mathbf{l}'}^{1/2} C_{\mathbf{k}'\mathbf{l}'} \sum_{\mathbf{i}} \bar{\phi}_{\mathbf{k}'\mathbf{i}} \phi_{\mathbf{l}'\mathbf{i}} - \lambda_{\mathbf{k}}^2 C_{\mathbf{k}\mathbf{k}} \quad (72)$$

$$= \lambda_{\mathbf{k}} \sum_{\mathbf{l}} \lambda_{\mathbf{l}} C_{\mathbf{l}\mathbf{l}} - \lambda_{\mathbf{k}}^2 C_{\mathbf{k}\mathbf{k}}, \quad (73)$$

matching desired Eq. (6) with  $\tau = 1$ .

Now we comment on the degenerate case, when  $\lambda_{\mathbf{k}} = 0$  for some  $\mathbf{k}$ . This occurs if there is linear dependence between some  $\psi(\mathbf{x}_i)$ , i.e.  $\dim \text{Ran}(\mathbf{H}) < N$ . The vectors  $\mathbf{u}_{\mathbf{k}}$  given by (68) with  $\lambda_{\mathbf{k}} \neq 0$  form a basis in  $\text{Ran}(\mathbf{H})$ . Inverse relation (69) remains valid with arbitrary vectors  $\mathbf{u}_{\mathbf{k}}$  for  $\mathbf{k}$  such that  $\lambda_{\mathbf{k}} = 0$  (this can be seen, for example, by lifting the degeneracy of the problem with a regularization  $\varepsilon$  and then letting  $\varepsilon \rightarrow 0$ ). As a result, Eq. (73) remains valid for  $\mathbf{k}$  such that  $\lambda_{\mathbf{k}} > 0$ . On the other hand, if  $\mathbf{u}_{\mathbf{k}}$  is an eigenvector corresponding to the eigenvalue  $\lambda_{\mathbf{k}} = 0$ , i.e.  $\mathbf{u}_{\mathbf{k}} \in \ker \mathbf{H}$ , then  $\mathbf{u}_{\mathbf{k}}$  is orthogonal to  $\psi(\mathbf{x}_i)$  for all  $\mathbf{i}$  and both formulas (5) and (6) yield  $(\widehat{D}\mathbf{C})_{kk} = 0$  for such  $k$ .  $\square$

## D Generating functions and their applications

### D.1 Reduction to generating functions

The derivations in Section 3 are evident except for the expansions (17), (19) of the noise and signal generating functions  $\tilde{U}(z)$ ,  $\tilde{V}(z)$  as series of scalar rational functions, which we now explain. Consider first expansion (17) for  $\tilde{U}(z)$ . The terms of this expansion correspond to the eigenvalues  $\lambda_k$  of  $\mathbf{H}$ . For each eigenvalue, the respective term is, by Eq. (16),

$$\lambda^2 \langle (\begin{smallmatrix} 1 & 0 \\ 0 & 0 \end{smallmatrix}), (1 - zA_\lambda)^{-1} (\begin{smallmatrix} 1 & 1 \\ 1 & 1 \end{smallmatrix}) \rangle, \quad (74)$$

where  $A_\lambda$  is the linear operator acting on the space of  $2 \times 2$  matrices and given by Eq. (10). The scalar product in (74) can be computed as the component  $x_{11}$  of the solution of the  $4 \times 4$  linear system

$$(1 - zA_\lambda) \begin{pmatrix} x_{11} & x_{12} \\ x_{21} & x_{22} \end{pmatrix} = \begin{pmatrix} 1 & 1 \\ 1 & 1 \end{pmatrix}. \quad (75)$$

Since all the components of the  $4 \times 4$  matrix of the operator  $1 - zA_\lambda$  are polynomial in the parameters  $\alpha, \beta, \gamma, \tau, \lambda, z$ , the resulting  $x_{11}$  is a rational function of these parameters. The explicit form of  $x_{11}$  is tedious to derive by hand, but it can be easily obtained with the help of a computer algebra system such as Sympy [31]. We provide the respective Jupyter notebook in the supplementary material.<sup>1</sup>

The terms of  $\tilde{V}$  are obtained similarly, but by solving the equation

$$(1 - zA_\lambda) \begin{pmatrix} x_{11} & x_{12} \\ x_{21} & x_{22} \end{pmatrix} = \begin{pmatrix} 1 & 0 \\ 0 & 0 \end{pmatrix} \quad (76)$$

instead of Eq. (75).

### D.2 Convergence conditions

**Proof of Proposition (3).** Note first that Proposition (3) is implied by the following lemma:

**Lemma 1.** *Assume (as in Proposition (3)) that  $\beta \in (-1, 1)$ ,  $0 < \alpha < 2(\beta + 1)/\lambda_{\max}$  and  $\gamma \in [0, 1]$ . Then*

1.  $S(\alpha, \beta, \gamma, \lambda, z) > 0$  for all  $z \in (0, 1)$ ;
2.  $\tilde{U}(z)$ ,  $\tilde{V}(z)$  are analytic in an open neighborhood of the interval  $(0, 1)$  and have no singularities there;
3.  $z\tilde{U}(z)$  is monotone increasing for all  $z \in (0, 1)$ .

Indeed, by statement 2) and representation (15), a singularity of  $\tilde{L}(z) = \tilde{V}(z)/(2(1 - z\tilde{U}(z)))$  on the interval  $(0, 1)$  can only be a pole resulting from a zero of the denominator  $1 - z\tilde{U}(z)$ . By statement 3), such a zero is present if and only if  $\tilde{U}(z) > 1$ , as claimed. It remains to prove the lemma.

*Proof of Lemma 1.*

1) Our proof of statement 1 is computer-assisted. Note first that this statement can be written as the condition  $W = \emptyset$  for a semi-algebraic set  $W \subset \mathbb{R}^4$  defined by several polynomial inequalities with integer coefficients:

$$W = \{ \exists (a, \beta, \gamma, z) \in \mathbb{R}^4 : (-1 < \beta < 1) \wedge (0 < a < 2(\beta + 1)) \quad (77)$$

$$\wedge (0 \leq \gamma \leq 1) \wedge (0 < z < 1) \wedge (S(a, \beta, \gamma, 1, z) \leq 0) \}, \quad (78)$$

where we have introduced the variable  $a = \alpha\lambda$ . By Tarski-Seidenberg theorem, the emptiness of a semi-algebraic set in  $\mathbb{R}^n$  is an algorithmically decidable problem (solvable by sequential elimination of existential quantifiers, via repeated standard operations such as differentiation, evaluation of polynomials, division of polynomials with remainder, etc., see e.g. [4]). This procedure is implemented in some computer algebra systems, e.g. in REDUCE/Redlog [13]. We used this system to verify that  $W = \emptyset$ :

<sup>1</sup><https://colab.research.google.com/drive/1eai1apCMCeLLbGIC7vfjbXN0KZ3CaIbw?usp=sharing>

```

1: rlset reals$
2: S := a**2*b*g*z**2 + a**2*b*z**2 + a**2*g*z - a**2*z - 2*a*b**2*z**2 -
2*a*b*z**2 + 2*a*b*z + 2*a*z - b**3*z**3 + b**3*z**2 + b**2*z**2 - b**2*z
+ b*z**2 - b*z - z + 1$
3: W := ex({a,b,g,z}, -1<b and b<1 and 0<a and a<2*(b+1) and 0<=g and g<=1
and 0<z and z<1 and S<=0)$
4: rlqe W;
false

```

2) Statement 2 follows from statement 1 and the fact that  $S(\alpha, \beta, \gamma, \lambda, z) \rightarrow (1-z)(1-\beta z)(1-\beta^2 z)$  as  $\lambda \rightarrow 0$ . Indeed, since the series  $\sum_k \lambda_k^2$  and  $\sum_k \lambda_k C_{kk,0}$  converge, singularities in  $\tilde{U}, \tilde{V}$  outside the points  $z = 1, \beta^{-1}, \beta^{-2}$  can only be poles of some of the terms of expansions (17), (19) associated with zeros of  $S$ , which are excluded by statement 1.

3) Our proof of statement 3 is also computer-assisted and similar to the proof of statement 1. First we compute

$$\frac{d}{dz}(z\tilde{U}(z)) = \gamma\alpha^2 \sum_k \lambda_k^2 \frac{R(\alpha, \beta, \lambda_k, z)}{S^2(\alpha, \beta, \gamma, \lambda_k, z)}, \quad (79)$$

where

$$R(\alpha, \beta, \lambda_k, z) = -2\alpha^2\beta\lambda_k^2z^2 + 4\alpha\beta^2\lambda_kz^2 + 4\alpha\beta\lambda_kz^2 + \beta^4z^4 + 2\beta^3z^3 - 2\beta^3z^2 - 2\beta^2z^2 - 2\beta z^2 + 2\beta z + 1. \quad (80)$$

By statement 1, it is sufficient to check that  $R \geq 0$  on the domain of interest. This is done by verifying the emptiness of the set

$$W_1 = \{\exists(a, \beta, z) \in \mathbb{R}^3 : (-1 < \beta < 1) \wedge (0 < a < 2(\beta + 1)) \quad (81)$$

$$\wedge (0 < z < 1) \wedge (R(a, \beta, 1, z) < 0)\} \quad (82)$$

in REDUCE/Redlog:

```

1: rlset reals$
2: R1 := -2*a**2*b*z**2 + 4*a*b**2*z**2 + 4*a*b*z**2 + b**4*z**4
+ 2*b**3*z**3 - 2*b**3*z**2 - 2*b**2*z**2 - 2*b*z**2 + 2*b*z + 1$
3: W1 := ex({a,b,z}, -1<b and b<1 and 0<a and a<2*(b+1) and 0<z and z<1
and R1<0)$
4: rlqe W1;
false

```

□

We provide experimental verifications of statements 1 and 2 in the accompanying Jupyter notebook.

### D.3 Loss asymptotic under power-laws

The main purpose of this section is to prove theorem 1. We first formulate a lemma allowing to calculate the  $\varepsilon \rightarrow +0$ ,  $\varepsilon = 1 - z$  asymptotics of the generating functions (17) and (19).

**Lemma 2.** *Suppose that  $S_k$  and  $C_k$  are two sequences such that  $S_k = k^{-\nu}(1 + o(1))$  and  $F_k = \sum_{l=k}^{\infty} C_l = k^{-\varkappa}(1 + o(1))$  as  $k \rightarrow \infty$ , with some constants  $\nu, \varkappa > 0$ . Also denote  $\zeta = \frac{\varkappa}{\nu}$ . Then*

1.

$$\sum_{l=k}^{\infty} C_l S_l = \frac{\zeta}{\zeta + 1} k^{-\varkappa - \nu} (1 + o(1)), \quad k \rightarrow \infty. \quad (83)$$

2. Assume  $\zeta < n$  for some  $n > 0$ , then

$$\sum_{k=1}^{\infty} \frac{C_k}{(\varepsilon + S_k)^n} = \frac{\Gamma(\zeta + 1)\Gamma(n - \zeta)}{\Gamma(n)} \varepsilon^{\zeta - n} (1 + o(1)), \quad \varepsilon \rightarrow 0 +. \quad (84)$$

*Proof.*

**Part 1.** Fix  $k$  and consider a discrete measure  $\mu_k$  with atoms located at points  $x_{l,k} = (l/k)^{-\nu}$ :

$$\mu_k = k^{\varkappa} \sum_{l=k}^{\infty} C_l \delta_{x_{l,k}} \quad (85)$$

By assumption on  $F_k$  as  $k \rightarrow \infty$ , the cumulative distribution function of  $\mu_k$  converges to cumulative distribution function of measure  $\mu(dx) = \mathbf{1}_{[0,1]} dx^{\zeta}$ , i.e. the measure  $\mu_k$  weakly converges to  $\mu$ .

Next, consider the function  $f_k(x)$  defined at points  $x_{l,k}$  by  $f_k(x_{l,k}) = k^{\nu} S_l$ , with  $f_k(0) = 0$ , linearly interpolated between the points  $x_{l,k}$ , and with  $f(x > 1) = f(x_{k,k})$ . Then  $f_k(x)$  converges uniformly on  $[0, 1]$  to  $f(x) = x$  as  $k \rightarrow \infty$ .

The above two observations on  $\mu_k$  and  $f_k$  give

$$\lim_{k \rightarrow \infty} k^{\varkappa + \nu} \sum_{l=k}^{\infty} C_l S_l = \lim_{k \rightarrow \infty} \int_0^1 f_k(x) \mu_k(dx) = \int_0^1 x \zeta x^{\zeta - 1} dx = \frac{\zeta}{\zeta + 1} \quad (86)$$

**Part 2.** For any  $a > 0$  let  $k_{a,\varepsilon} = \lfloor (\varepsilon a)^{-1/\nu} \rfloor$ . Rescale the sum of interest and divide it into two parts separated by index  $k_{a,\varepsilon}$ :

$$\varepsilon^{n - \zeta} \sum_{k=1}^{\infty} \frac{C_k}{(\varepsilon + S_k)^n} = \varepsilon^{n - \zeta} \sum_{k=1}^{k_{a,\varepsilon}} + \varepsilon^{n - \zeta} \sum_{k=k_{a,\varepsilon}+1}^{\infty} =: I_1(a, \varepsilon) + I_2(a, \varepsilon). \quad (87)$$

We will show that

$$\limsup_{\varepsilon \rightarrow 0+} I_1(a, \varepsilon) = O(a^{\zeta - n}), \quad (88)$$

$$\lim_{\varepsilon \rightarrow 0+} I_2(a, \varepsilon) = \int_0^a \frac{dx^{\zeta}}{(1+x)^n} =: J(a). \quad (89)$$

These two fact will imply the statement of the lemma since  $\zeta - n < 0$  and

$$\lim_{a \rightarrow +\infty} J(a) = \int_0^{\infty} \frac{\zeta x^{\zeta - 1}}{(1+x)^n} dx \quad (90)$$

$$\stackrel{1+x=1/t}{=} \zeta \int_0^1 t^{n - \zeta - 1} (1-t)^{\zeta - 1} dt \quad (91)$$

$$= \zeta B(n - \zeta, \zeta). \quad (92)$$



To prove Eq. (88), use summation by parts and the hypotheses on  $S_k, F_k$ :

$$\varepsilon^{n-\zeta} \sum_{k=1}^{k_{a,\varepsilon}} \frac{C_k}{(\varepsilon + S_k)^n} = \varepsilon^{n-\zeta} O\left(\sum_{k=1}^{k_{a,\varepsilon}} C_k k^{\nu n}\right) \quad (93)$$

$$= \varepsilon^{n-\zeta} O\left(\sum_{k=1}^{k_{a,\varepsilon}} (F_k - F_{k+1}) k^{\nu n}\right) \quad (94)$$

$$= \varepsilon^{n-\zeta} O\left(F_1 - F_{k_{a,\varepsilon}+1} k_{a,\varepsilon}^{\nu n} + \sum_{k=2}^{k_{a,\varepsilon}} F_k (k^{\nu n} - (k-1)^{\nu n})\right) \quad (95)$$

$$= \varepsilon^{n-\zeta} O(k_{a,\varepsilon}^{\nu n - \kappa}) \quad (96)$$

$$= O(a^{\zeta - n}). \quad (97)$$

To prove Eq. (89), it is convenient to represent the sum  $I_2(a, \varepsilon)$  as an integral over discrete measure  $\mu_{a,\varepsilon}$  with atoms  $x_{k,\varepsilon} = k^{-\nu}/\varepsilon$ :

$$I_2(a, \varepsilon) = \int f_\varepsilon d\mu_{a,\varepsilon}(x), \quad (98)$$

$$\mu_{a,\varepsilon} = \varepsilon^{-\zeta} \sum_{k=k_{a,\varepsilon}+1}^{\infty} C_k \delta_{x_{k,\varepsilon}}, \quad (99)$$

$$f_\varepsilon(x_{k,\varepsilon}) = (1 + S_k/\varepsilon)^{-n}. \quad (100)$$

Again, by assumption on  $F_k$ , as  $\varepsilon \rightarrow 0+$ , the cumulative distribution functions of  $\mu_{a,\varepsilon}$  converge to the cumulative distribution function of the measure  $\mu_a(dx) = \mathbf{1}_{[0,a]} dx^\zeta$ , i.e., the measures  $\mu_{a,\varepsilon}$  weakly converge to  $\mu_a$ . At the same time, the functions  $f_\varepsilon(x)$  converge to  $(1+x)^{-n}$  uniformly on  $[0, a]$ . This implies desired convergence (89).  $\square$

Now we are ready to proceed with the proof of theorem 1.

**Theorem 1.** Assume spectral conditions (23) with  $\nu > 1$  and that parameters  $\alpha, \beta, \gamma$  are as in Proposition 3 and such that convergence condition  $\tilde{U}(1) < 1$  is satisfied. Then

$$\sum_{t=1}^T tL(t) = (1 + o(1)) \begin{cases} \frac{K\Gamma(\zeta+1)}{2(1-\tilde{U}(1))(2-\zeta)} \left(\frac{2\alpha\Lambda}{1-\beta}\right)^{-\zeta} t^{2-\zeta}, & 2-\zeta > 1/\nu, \\ \frac{\gamma\tilde{V}(1)\Gamma(2-1/\nu)}{8(1-\tilde{U}(1))^2} \left(\frac{2\alpha\Lambda}{1-\beta}\right)^{1/\nu} t^{1/\nu}, & 2-\zeta < 1/\nu. \end{cases} \quad (24)$$

*Proof.* As asymptotic of partial sums  $\sum_{t=1}^T tL(t)$  are associated with asymptotic of  $\tilde{L}'(1-\varepsilon)$  at  $\varepsilon \rightarrow +0$  we recall its expression (25)

$$\frac{d}{dz} \tilde{L}(z) = \frac{\frac{d}{dz} \tilde{V}(z)}{2(1-z\tilde{U}(z))} + \frac{\tilde{V}(z) \frac{d}{dz}(z\tilde{U}(z))}{2(1-z\tilde{U}(z))^2} \quad (101)$$

Full expressions for generating functions (17) and (19) can be significantly simplified in the limit  $\varepsilon \rightarrow +0$  and  $\lambda_k \rightarrow 0$

$$\tilde{U}(1-\varepsilon) = \gamma \sum_{k=1}^{\infty} \frac{\left(\frac{\alpha\lambda_k}{1-\beta}\right)^2}{\varepsilon + 2\frac{\alpha\lambda_k}{1-\beta}} (1 + O(\lambda_k) + O(\varepsilon)) \quad (102)$$

$$\tilde{V}(1-\varepsilon) = \sum_{k=1}^{\infty} \frac{\lambda_k C_{kk}}{\varepsilon + 2\frac{\alpha\lambda_k}{1-\beta}} (1 + O(\lambda_k) + O(\varepsilon)) \quad (103)$$

Differentiating we get

$$\tilde{U}'(1-\varepsilon) = \gamma \sum_{k=1}^{\infty} \frac{\left(\frac{\alpha\lambda_k}{1-\beta}\right)^2}{\left(\varepsilon + 2\frac{\alpha\lambda_k}{1-\beta}\right)^2} (1 + O(\lambda_k) + O(\varepsilon)) \quad (104)$$

$$\tilde{V}'(1-\varepsilon) = \sum_{k=1}^{\infty} \frac{\lambda_k C_{kk}}{\left(\varepsilon + 2\frac{\alpha\lambda_k}{1-\beta}\right)^2} (1 + O(\lambda_k) + O(\varepsilon)) \quad (105)$$

Let's make a couple of observations. From asymptotic expressions above one can show that

$$\tilde{U}(1-\varepsilon) \sim \sum_{k=1}^{\infty} \frac{\lambda_k^2}{\varepsilon + \lambda_k} \sim \sum_{k=1}^{\varepsilon^{-\frac{1}{\nu}}} \lambda_k \sim 1 \quad (106)$$

$$\tilde{U}'(1-\varepsilon) \sim \sum_{k=1}^{\infty} \frac{\lambda_k^2}{(\varepsilon + \lambda_k)^2} \sim \sum_{k=1}^{\varepsilon^{-\frac{1}{\nu}}} 1 \sim \varepsilon^{-\frac{1}{\nu}} \quad (107)$$

$$\tilde{V}(1-\varepsilon) \sim \sum_{k=1}^{\infty} \frac{\lambda_k C_{kk}}{\varepsilon + \lambda_k} \sim \sum_{k=1}^{\varepsilon^{-\frac{1}{\nu}}} C_{kk} \sim \begin{cases} 1, & \zeta > 1 \\ \varepsilon^{\zeta-1}, & \zeta < 1 \end{cases} \quad (108)$$

$$\tilde{V}'(1-\varepsilon) \sim \sum_{k=1}^{\infty} \frac{\lambda_k C_{kk}}{(\varepsilon + \lambda_k)^2} \sim \sum_{k=1}^{\varepsilon^{-\frac{1}{\nu}}} \frac{C_{kk}}{\lambda_k} \sim \begin{cases} 1, & \zeta > 2 \\ \varepsilon^{\zeta-2}, & \zeta < 2 \end{cases} \quad (109)$$

Here the sign  $\sim$  means an asymptotic ( $\varepsilon \rightarrow 0$ ) equality up to a multiplicative constant. Using these asymptotic relations we see that for  $\tilde{L}'(1-\varepsilon)$  leading asymptotic terms are given by either  $\tilde{U}'(1-\varepsilon)$  when  $\zeta > 2 - \frac{1}{\nu}$ , or by  $\tilde{V}'(1-\varepsilon)$  when  $\zeta < 2 - \frac{1}{\nu}$ .

Now we set for simplicity  $\Lambda = K = 1$  and apply lemma 2 to (104) and (105) to get more refined asymptotic expressions. For  $V'(1-\varepsilon)$  we assume  $\zeta < 2$  because  $V'(1-\varepsilon) = O(1)$  for  $\zeta > 2$  and refined asymptotic is not needed.

$$\begin{aligned} \tilde{V}'(1-\varepsilon) &= \sum_{k=1}^{\infty} \frac{\lambda_k C_{kk} (1 + O(\lambda_k) + O(\varepsilon))}{\left(\varepsilon + 2 \frac{\alpha \lambda_k}{1-\beta}\right)^2} \\ &= (1 + O(\varepsilon)) \sum_{k=1}^{\infty} \frac{\lambda_k C_{kk}}{\left(\varepsilon + 2 \frac{\alpha \lambda_k}{1-\beta}\right)^2} + \sum_{k=1}^{\infty} \frac{O(C_{kk} \lambda_k^2)}{\left(\varepsilon + 2 \frac{\alpha \lambda_k}{1-\beta}\right)^2} \\ &\stackrel{(1)}{=} \left(\frac{2\alpha}{1-\beta}\right)^{-2} \sum_{k=1}^{\infty} \frac{C_{kk} \lambda_k}{\left(\frac{\varepsilon(1-\beta)}{2\alpha} + \lambda_k\right)^2} + O(\varepsilon^{\min(0, \zeta-1)}) \\ &\stackrel{(1)}{=} \Gamma(\zeta+1) \Gamma(2-\zeta) \left(\frac{2\alpha}{1-\beta}\right)^{-\zeta} \varepsilon^{\zeta-2} (1 + o(1)) \end{aligned} \quad (110)$$

Here in (1) we first used first part of lemma 2 to get  $\sum_{l \geq k} C_{ll} \lambda_l^2 = \frac{\zeta}{\zeta+1} k^{-\zeta-\nu} (1 + o(1))$ . Then for  $1 < \zeta < 2$  the second sum is finite (see (109)) and for  $\zeta < 1$  second part of lemma 2 allows to bound the sum as  $O(\varepsilon^{\zeta-1})$ . In (2) we applied second part of lemma 2 to the first sum in (1).

For  $U'(1-\varepsilon)$  we have

$$\begin{aligned} \tilde{U}'(1-\varepsilon) &= \gamma \sum_{k=1}^{\infty} \frac{\left(\frac{\alpha \lambda_k}{1-\beta}\right)^2 (1 + O(\lambda_k) + O(\varepsilon))}{\left(\varepsilon + 2 \frac{\alpha \lambda_k}{1-\beta}\right)^2} \\ &\stackrel{(1)}{=} \frac{\gamma}{4} (1 + O(\varepsilon)) \sum_{k=1}^{\infty} \frac{\lambda_k^2}{\left(\frac{\varepsilon(1-\beta)}{2\alpha} + \lambda_k\right)^2} + \frac{\gamma}{4} \sum_{k=1}^{\infty} \frac{O(\lambda_k^3)}{\left(\frac{\varepsilon(1-\beta)}{2\alpha} + \lambda_k\right)^2} \\ &\stackrel{(2)}{=} \frac{\gamma}{4\nu} \Gamma(2 - \frac{1}{\nu}) \Gamma(\frac{1}{\nu}) \left(\frac{2\alpha}{1-\beta}\right)^{\frac{1}{\nu}} \varepsilon^{-\frac{1}{\nu}} (1 + o(1)) \end{aligned} \quad (111)$$

In (1) the second sum can be bounded as  $O(1)$  after recalling that  $\nu > 1$ . In (2) we again applied second part of lemma 2 with  $C_k = \lambda_k^2$  and  $n = 2$  since  $\sum_{l \geq k} \lambda_l^2 = \frac{1}{2\nu-1} k^{-2\nu+1} (1 + o(1))$ . To get the coefficient in (2) we used  $\frac{\Gamma(3-1/\nu)}{2\nu-1} = \frac{\Gamma(2-1/\nu)}{\nu}$ .

Substituting (111) and (110) into (101) we get

$$\tilde{L}'(1-\varepsilon) = \frac{C_{V'}}{2(1-\tilde{U}(1))} \varepsilon^{-\max(0, 2-\zeta)} (1 + o(1)) + \frac{\tilde{V}(1) C_{U'}}{2(1-\tilde{U}(1))^2} \varepsilon^{-\frac{1}{\nu}} (1 + o(1)) \quad (112)$$

where  $C_{V'}$  and  $C_{U'}$  are constants in the asymptotics (110) and (111). Picking the leading term depending on the sign of  $\zeta - (2 - \frac{1}{\nu})$  we obtain final expressions

$$\tilde{L}'(1 - \varepsilon) = \begin{cases} \frac{\Gamma(\zeta+1)\Gamma(2-\zeta)}{2(1-\tilde{U}(1))} \left(\frac{2\alpha}{1-\beta}\right)^{-\zeta} \varepsilon^{\zeta-2}(1+o(1)), & \zeta < 2 - \frac{1}{\nu} \\ \gamma \frac{\tilde{V}(1)\Gamma(2-\frac{1}{\nu})\Gamma(\frac{1}{\nu})}{8\nu(1-\tilde{U}(1))^2} \left(\frac{2\alpha}{1-\beta}\right)^{\frac{1}{\nu}} \varepsilon^{-\frac{1}{\nu}}(1+o(1)), & \zeta > 2 - \frac{1}{\nu} \end{cases} \quad (113)$$

The last step is to apply Tauberian theorem ([15], p. 445) which states that if generating function  $\tilde{F}(z)$  of a sequence  $F(t)$  has asymptotic  $\tilde{F}(1 - \varepsilon) = C\varepsilon^{-\rho}(1+o(1))$ , then the partial sums have the asymptotic  $\sum_{t=1}^T F(t) = \frac{C}{\Gamma(\rho+1)} T^\rho(1+o(1))$ . Applying this theorem to  $F(t) = tL(t)$  and its generating function given by (113) we get precisely (24) with  $\Lambda = K = 1$ . To restore the values of constants  $\Lambda, K$  recall that the part of the loss coming from signal ( $\tilde{V}(z)$ ) is simply proportional to  $K$ , and  $\Lambda$  always goes in combination  $\alpha\Lambda$ .  $\square$

Finally, let us show how (24) can be used to obtain asymptotics (26a),(26b) for the loss values  $L(t)$  themselves. Assuming that  $L(t) = Ct^{-\xi}$ ,  $\xi < 2$ , we get

$$\sum_{t=1}^T tL(t) = C \sum_{t=1}^T t^{-\xi+1}(1+o(1)) \approx C \int_1^T t^{-\xi+1}(1+o(1)) = \frac{C}{2-\xi} T^{2-\xi}(1+o(1)) \quad (114)$$

Comparing this with (24), we find the constants  $C$  appearing in (26a),(26b).

#### D.4 Exponential divergence of the loss and convergence-divergence transition

**Convergence radius  $r_L$  and exponential divergence rate.** By Proposition 3, the convergence radius  $r_L < 1$  if and only if  $\tilde{U}(1) > 1$ , and in the case  $\tilde{U}(1) > 1$  it is determined by the condition

$$1 = r_L \tilde{U}(r_L). \quad (115)$$

If  $r_L < 1$ , loss exponentially diverges as  $t \rightarrow \infty$ :

**Proposition 5.** *Under assumption of Proposition 3, suppose that  $r_L < 1$ . Then*

$$\sum_{t=0}^T L(t)r_L^t = \frac{\tilde{V}(r_L)}{2(1+r_L^2\tilde{U}'(r_L))} T(1+o(1)), \quad (T \rightarrow \infty). \quad (116)$$

*Proof.* Consider the modified generating function  $\tilde{L}_1(z) = \tilde{L}(r_L z)$ , which is the generating function for the sequence  $L(t)r_L^t$ :

$$\tilde{L}_1(z) = \sum_{t=0}^{\infty} z^t L(t)r_L^t. \quad (117)$$

The convergence radius for  $\tilde{L}_1$  is 1. We can also write

$$\tilde{L}_1(1 - \epsilon) = \frac{\tilde{V}(r_L(1 - \epsilon))}{2(1 - r_L(1 - \epsilon)\tilde{U}(r_L(1 - \epsilon)))} \quad (118)$$

$$= \frac{\tilde{V}(r_L)}{2(1 + r_L^2\tilde{U}'(r_L))\epsilon} (1 + o(1)), \quad (\epsilon \rightarrow 0). \quad (119)$$

The statement of the proposition then follows by the Tauberian theorem.  $\square$

If we assume that

$$L(t) \sim Cr_L^{-t} \quad (120)$$

with some constant  $C$ , then this constant is fixed by Eq. (116):

$$L(t) \sim \frac{\tilde{V}(r_L)}{2(1 + r_L^2\tilde{U}'(r_L))} r_L^{-t}. \quad (121)$$

**“Eventual divergence” phase with small  $\alpha$ .** Recall that we characterized the “eventual divergence” phase by the condition  $\tilde{U}(1) = \infty$ . In this phase we necessarily have  $r_L < 1$ . However,  $r_L$  can be very close to 1 (and thus “divergence delayed”) – for example if the learning rate  $\alpha$  is very small. In this scenario we can derive an asymptotic expression for the difference  $\epsilon_* = 1 - r_L$ .

In the sequel, we assume for simplicity that  $\beta = 0$  and  $\tau = \gamma = 1$ , and that the eigenvalues and initial covariance coefficients  $C_{kk,0}$  satisfy power law relations (23) with  $\frac{1}{2} < \nu < 1$  (corresponding to the “eventual divergence” phase).

**Proposition 6.** As  $\alpha \rightarrow 0$ ,

$$\epsilon_* \equiv 1 - r_L = \left( \frac{1}{4\nu} \Gamma(2 - 1/\nu) \Gamma(1/\nu - 1) \right)^{\nu/(1-\nu)} (2\alpha\Lambda)^{1/(1-\nu)} (1 + o(1)). \quad (122)$$

*Proof.* With  $\beta = 0$  and  $\tau = \gamma = 1$ , we have by Eq. (17)

$$\tilde{U}(1 - \epsilon) = \alpha^2 \sum_k \frac{\lambda_k^2}{2\alpha\lambda_k(1 - \epsilon) + \epsilon} \quad (123)$$

$$= \frac{\alpha}{2\Lambda} \sum_k \frac{\lambda_k^2 / (1 - 2\alpha\lambda_k)}{\lambda_k / (\Lambda(1 - 2\alpha\lambda_k)) + \epsilon / (2\alpha\Lambda)}. \quad (124)$$

For any  $\alpha$ , we can now apply Lemma 2(2) with  $\varkappa = 2\nu - 1$ ,  $\zeta = 2 - 1/\nu$  and  $n = 1$  and get

$$\tilde{U}(1 - \epsilon) = \frac{\alpha\Lambda}{2(2\nu - 1)} \Gamma(3 - 1/\nu) \Gamma(1/\nu - 1) \left( \frac{\epsilon}{2\alpha\Lambda} \right)^{1-1/\nu} (1 + o(1)) \quad (125)$$

$$= \frac{1}{4\nu} \Gamma(2 - 1/\nu) \Gamma(1/\nu - 1) (2\alpha\Lambda)^{1/\nu} \epsilon^{1-1/\nu} (1 + o(1)), \quad (\epsilon \rightarrow 0). \quad (126)$$

It is easy to see that  $o(1)$  here is uniform for small  $\alpha$ . The desired  $\epsilon_* = \epsilon_*(\alpha)$  is determined from the equation  $1 = (1 - \epsilon_*)\tilde{U}(1 - \epsilon_*)$ . As  $\alpha \rightarrow 0$ , we clearly have  $\epsilon_* = \epsilon_*(\alpha) \rightarrow 0$ . It follows that

$$1 = \frac{1}{4\nu} \Gamma(2 - 1/\nu) \Gamma(1/\nu - 1) (2\alpha\Lambda)^{1/\nu} \epsilon_*^{1-1/\nu} (1 + o(1)), \quad (\alpha \rightarrow 0). \quad (127)$$

This implies desired expression (122).  $\square$

We can similarly use Lemma 2 to also estimate the derivative  $\tilde{U}'(1 - \epsilon)$  :

$$\tilde{U}'(1 - \epsilon) = \alpha^2 \sum_k \frac{\lambda_k^2 (1 - 2\alpha\lambda_k)}{(2\alpha\lambda_k(1 - \epsilon_*) + \epsilon)^2} \quad (128)$$

$$= \frac{1}{4\Lambda^2} \sum_k \frac{\lambda_k^2 / (1 - 2\alpha\lambda_k)}{(\lambda_k / (\Lambda(1 - 2\alpha\lambda_k)) + \epsilon / (2\alpha\Lambda))^2} \quad (129)$$

$$= \frac{1}{4(2\nu - 1)} \Gamma(3 - 1/\nu) \Gamma(1/\nu) \left( \frac{\epsilon}{2\alpha\Lambda} \right)^{-1/\nu} (1 + o(1)) \quad (130)$$

$$= \frac{1}{4\nu} \Gamma(2 - 1/\nu) \Gamma(1/\nu) (2\alpha\Lambda)^{1/\nu} \epsilon^{-1/\nu} (1 + o(1)) \quad (131)$$

$$= \frac{1/\nu - 1}{\epsilon} \tilde{U}(1 - \epsilon) (1 + o(1)), \quad (\epsilon \rightarrow 0) \quad (132)$$

(this result can also formally be obtained by differentiating Eq. (125) in  $\epsilon$ ). In particular, for  $\epsilon = \epsilon_*$  we get

$$\tilde{U}'(1 - \epsilon_*) = \frac{1/\nu - 1}{\epsilon_* r_L} (1 + o(1)), \quad (\alpha \rightarrow 0). \quad (133)$$

**“Early convergent” regime.** If  $r_L < 1$ , then, as discussed above, loss eventually diverges exponentially. However, in general, we expect this divergence to occur only after some interval of convergence (see Figure 3(right)). We will give the loss asymptotic for this “early convergent” phase and give a rough estimate of the time scale at which the transition between the two regimes occurs.

We retain the assumptions  $\beta = 0$  and  $\gamma = \tau = 1$  from the previous paragraph, and assume power laws (23) with  $\frac{1}{2} < \nu < 1$  and  $\zeta < 1$ .

We start with finding the loss asymptotic in the early convergent phase. First we argue that this phase can be approximately described by the loss generating function

$$\tilde{L}(z) \approx \frac{1}{2} \tilde{V}(z), \quad (134)$$

i.e. generating function (15) in which we approximate the denominator by 1:

$$1 - z\tilde{U}(z) \approx 1. \quad (135)$$

This approximation can be justified for  $z < r_L$  by noting that, by Eq. (125),

$$\tilde{U}(1 - \epsilon) \approx \left(\frac{\epsilon}{\epsilon_*}\right)^{1-1/\nu} \tilde{U}(1 - \epsilon_*) = \left(\frac{\epsilon}{\epsilon_*}\right)^{1-1/\nu} \quad (136)$$

with  $1 - 1/\nu < 0$ . We remark that approximations (135) and (134) essentially mean that we ignore terms containing factors  $U_{t,s}$  associated with noise in expansion (11).

If relation (134) held for all  $z \in (0, 1)$ , then we would have an asymptotic convergence of the loss for all  $t$ . Indeed, under our assumptions,

$$\tilde{V}(1 - \epsilon) = \sum_{k=1}^{\infty} \frac{\lambda_k C_{kk,0}}{2\alpha\lambda_k(1 - \epsilon) + \epsilon} \quad (137)$$

and  $\tilde{V}(1 - \epsilon) \rightarrow \infty$  as  $\epsilon \rightarrow 0$  (since  $\zeta < 1$ ). Applying again Lemma 2, we find

$$\tilde{V}(1 - \epsilon) = \frac{1}{2\alpha\Lambda} \sum_k \frac{\lambda_k C_{kk,0}/(1 - 2\alpha\lambda_k)}{\lambda_k/(\Lambda(1 - 2\alpha\lambda_k)) + \epsilon/(2\alpha\Lambda)} \quad (138)$$

$$= \frac{K}{2\alpha\Lambda} \Gamma(\zeta + 1) \Gamma(1 - \zeta) \left(\frac{\epsilon}{2\alpha\Lambda}\right)^{\zeta-1} (1 + o(1)) \quad (139)$$

$$= \frac{K}{2} \Gamma(\zeta + 1) \Gamma(1 - \zeta) (2\alpha\Lambda)^{-\zeta} \epsilon^{\zeta-1} (1 + o(1)), \quad (\epsilon \rightarrow 0). \quad (140)$$

The Tauberian theorem then implies that

$$\sum_{t=0}^T L(t) = \frac{K}{2\Gamma(2 - \zeta)} \Gamma(\zeta + 1) \Gamma(1 - \zeta) (2\alpha\Lambda)^{-\zeta} T^{1-\zeta} (1 + o(1)) \quad (141)$$

$$= \frac{K}{2(1 - \zeta)} \Gamma(\zeta + 1) (2\alpha\Lambda)^{-\zeta} T^{1-\zeta} (1 + o(1)), \quad (\epsilon \rightarrow 0). \quad (142)$$

Assuming a power-law form

$$L(t) \sim Ct^{-\zeta}, \quad (143)$$

we then find

$$L(t) \sim \frac{K}{2} \Gamma(\zeta + 1) (2\alpha\Lambda)^{-\zeta} t^{-\zeta}. \quad (144)$$

This expression agrees with “signal-dominated” loss asymptotic (26a) up to the factor  $(1 - \tilde{U}(1))^{-1}$  (missing because of our approximation (135)).

**Transition from convergence to divergence.** Of course, the obtained asymptotic (144) does not hold for very large  $t$ , since representation (134) breaks down at  $z \gtrsim r_L$ , and the loss trajectory switches to exponential divergence. We can roughly estimate the switching time  $t_{\text{blowup}}$  by equating the asymptotic expressions for  $L(t)$  in the convergent and divergent phases:

$$\frac{K}{2} \Gamma(\zeta + 1) (2\alpha\Lambda)^{-\zeta} t_{\text{blowup}}^{-\zeta} \approx \frac{\tilde{V}(r_L)}{2(1 + r_L^2 \tilde{U}'(r_L))} r_L^{-t_{\text{blowup}}}. \quad (145)$$

This is a transcendental equation not explicitly solvable in  $t_{\text{blowup}}$ . We simplify it using a number of approximations. Using approximation (140) for  $\tilde{V}(r_L)$  and the fact that  $\epsilon_*$  is small, we can simplify this equation to

$$\frac{1 + r_L^2 \tilde{U}'(1 - \epsilon_*)}{\Gamma(1 - \zeta)} \epsilon_*^{1-\zeta} t_{\text{blowup}}^{-\zeta} \approx (1 - \epsilon_*)^{-t_{\text{blowup}}} \approx e^{\epsilon_* t_{\text{blowup}}}. \quad (146)$$

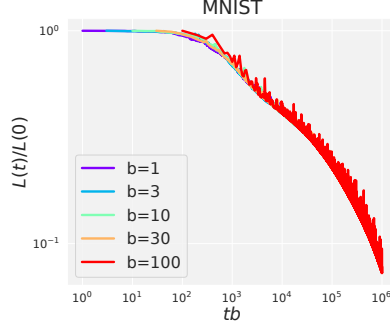


Figure 5: Representation of loss  $L(t)$  obtained using different batch sizes  $b$  as (approximately) a function of the computation budget  $bt$  (regardless of how it is factorized over  $b$  and  $t$ ) for MNIST. Momentum is fixed at  $\beta = 0$  and the ratio  $\alpha/b$  is kept the same for all curves.

Next, using Eq. (133), we can approximate the l.h.s. by

$$\frac{1 + r_L^2 \tilde{U}'(1 - \epsilon_*)}{\Gamma(1 - \zeta)} \epsilon_*^{1-\zeta} t_{\text{blowup}}^{-\zeta} \approx \frac{1/\nu - 1}{\Gamma(1 - \zeta)} \epsilon_*^{-\zeta} t_{\text{blowup}}^{-\zeta}. \quad (147)$$

It follows that Eq. (146) can be approximated as

$$\frac{1/\nu - 1}{\Gamma(1 - \zeta)} (\epsilon_* t_{\text{blowup}})^{-\zeta} = e^{\epsilon_* t_{\text{blowup}}}. \quad (148)$$

Thus, we can write

$$t_{\text{blowup}} \approx \frac{a_*}{\epsilon_*}, \quad (149)$$

where  $a_*$  is the solution of the equation

$$\frac{1/\nu - 1}{\Gamma(1 - \zeta)} a_*^{-\zeta} = e^{a_*}. \quad (150)$$

If  $t_{\text{div}} = -1/\log r_L$  denotes the characteristic time scale of exponential divergence, then at small  $\alpha$  we have  $t_{\text{div}} \approx 1/\epsilon_*$ , so the characteristic transition time  $t_{\text{blowup}}$  is related to  $t_{\text{div}}$  by the simple relation

$$t_{\text{blowup}} \approx a_* t_{\text{div}}. \quad (151)$$

## D.5 Budget optimization

Figure 5 shows that the loss is, approximately, a function of total computation budget given by the product  $bt$ , regardless of specific values of  $b$  and  $t$ . See [30, 41] for general discussions of batch scalability.

## D.6 Negative momenta

Our analysis of the effect of momentum is based on the approximations (26a), (26b) for  $L(t)$  at large  $t$ . Let us denote these approximations by  $L_{\text{approx}}(t)$ :

$$L(t) \approx L_{\text{approx}}(t) := \begin{cases} \frac{K\Gamma(\zeta+1)}{2(1-\tilde{U}(1))} \left(\frac{2\alpha\Lambda}{1-\beta}\right)^{-\zeta} t^{-\zeta}, & \zeta < 2 - 1/\nu, \end{cases} \quad (152a)$$

$$\begin{cases} \frac{\gamma\tilde{V}(1)\Gamma(2-1/\nu)}{8\nu(1-\tilde{U}(1))^2} \left(\frac{2\alpha\Lambda}{1-\beta}\right)^{1/\nu} t^{1/\nu-2}, & \zeta > 2 - 1/\nu. \end{cases} \quad (152b)$$

We can now formulate a rigorous result on how  $L_{\text{approx}}(t)$  is affected by changing the momentum from  $\beta = 0$  at the optimal  $\alpha$ . Note that  $t$  enters expression  $L_{\text{approx}}(t)$  only through the factor  $t^{-\zeta}$  or  $t^{1/\nu-2}$ ; as a result, the statements below hold in the same form for all  $t > 0$ .

**Proposition 7.** *Suppose that the eigenvalues  $\lambda_k$  and initial moments  $C_{kk,0}$  are subject to large- $k$  power law asymptotics (23) with some exponents  $\nu, \kappa > 0$ ,  $\zeta = \kappa/\nu$  and coefficients  $\Lambda, K$ . Let  $\tau = \gamma = 1$ . Let  $\alpha_{\text{opt}} = \arg \min_{\alpha} L_{\text{approx}}(t)|_{\beta=0}$ .*

*1. (signal-dominated phase) If  $\zeta < 2 - 1/\nu$ , then*

1.  $\alpha_{\text{opt}} = \frac{2\zeta}{\zeta+1}(\sum_k \lambda_k)^{-1}$ ;
2.  $\partial_\beta L_{\text{approx}}(t)|_{\beta=0, \alpha=\alpha_{\text{opt}}} < 0$ .

**II. (noise-dominated phase)** If  $\zeta > 2 - 1/\nu$ , then

1.  $\alpha_{\text{opt}} = \frac{2(\nu-1)}{3\nu-1}(\sum_k \lambda_k)^{-1}$ ;
2. The sign of  $\partial_\beta L_{\text{approx}}(t)|_{\beta=0, \alpha=\alpha_{\text{opt}}}$  equals the sign of the expression

$$\nu \sum_k \lambda_k \sum_k \lambda_k C_{kk,0} - (\nu-1) \sum_k \lambda_k^2 \sum_k C_{kk,0} \quad (153)$$

(as in Eq. (28)).

Before giving the proof, note that if  $\beta = 0$  then, by Eq. (20), our main stability condition  $\tilde{U}(1) \leq 1$  (see Prop. 3) becomes simply

$$\alpha \leq \alpha_{\text{max}} := 2 \left( \sum_k \lambda_k \right)^{-1}. \quad (154)$$

It follows that  $\alpha_{\text{opt}}$  described in statements I1 and I2 belong to the allowed interval  $(0, \alpha_{\text{max}})$ .

*Proof of Proposition 7.*

**I. (signal-dominated phase)** Differentiating Eq. (152a) and denoting by  $\phi$  various (in general, different) positive values, we get

$$\partial_\alpha L_{\text{approx}}(t)|_{\beta=0} = \phi[(1 - \tilde{U}(z=1, \beta=0))\partial_\alpha \alpha^{-\zeta} + \alpha^{-\zeta} \partial_\alpha \tilde{U}(z=1, \beta=0)] \quad (155)$$

$$= \phi \alpha^{-\zeta} \left[ \left(1 - \frac{\alpha}{2} \sum_k \lambda_k\right) \frac{-\zeta}{\alpha} + \frac{1}{2} \sum_k \lambda_k \right] \quad (156)$$

$$= \phi \left[ \alpha \frac{\zeta+1}{2} \sum_k \lambda_k - \zeta \right], \quad (157)$$

implying statement 1:

$$\alpha_{\text{opt}} = \frac{2\zeta}{\zeta+1} \left( \sum_k \lambda_k \right)^{-1}. \quad (158)$$

Next,

$$\partial_\beta L_{\text{approx}}(t)|_{\beta=0} = \phi[(1 - \tilde{U}(z=1, \beta=0))\partial_\beta (1-\beta)^\zeta + (1-\beta)^\zeta \partial_\beta \tilde{U}(z=1, \beta=0)] \quad (159)$$

$$= \phi(1-\beta)^\zeta \left[ \left(1 - \frac{\alpha}{2} \sum_k \lambda_k\right) \frac{-\zeta}{1-\beta} + \frac{\alpha}{2} \sum_k \lambda_k (1 - \alpha \lambda_k) \right] \Big|_{\beta=0} \quad (160)$$

$$= \phi \left[ \left(1 - \frac{\alpha}{2} \sum_k \lambda_k\right)(-\zeta) + \frac{\alpha}{2} \sum_k \lambda_k (1 - \alpha \lambda_k) \right]. \quad (161)$$

Substituting  $\alpha = \alpha_{\text{opt}}$  we get

$$\partial_\beta L_{\text{approx}}(t)|_{\beta=0, \alpha=\alpha_{\text{opt}}} = \phi \left[ \left(1 - \frac{\zeta}{\zeta+1}\right)(-\zeta) + \frac{\zeta}{\zeta+1} \left(1 - \frac{\zeta}{\zeta+1} \left(\sum_k \lambda_k^2 \left(\sum_k \lambda_k\right)^{-1}\right)\right) \right] \quad (162)$$

$$= \phi \left[ - \left(\frac{\zeta}{\zeta+1}\right)^2 \left(\sum_k \lambda_k\right)^{-1} \sum_k \lambda_k^2 \right] \quad (163)$$

$$< 0, \quad (164)$$

proving statement 2.

**II. (noise-dominated phase)** Differentiating Eq. (152b),

$$\begin{aligned}\partial_\alpha L_{\text{approx}}(t)|_{\beta=0} &= \phi \left[ (1 - \tilde{U}(1)) [\tilde{V}(1) \partial_\alpha \alpha^{1/\nu} + \alpha^{1/\nu} \partial_\alpha \tilde{V}(1)] + 2\alpha^{1/\nu} \tilde{V}(1) \partial_\alpha \tilde{U}(1) \right] \Big|_{\beta=0} \\ &= \phi \left[ \left(1 - \frac{\alpha}{2} \sum_k \lambda_k\right) \left(\frac{1}{\nu\alpha} (2\alpha)^{-1} \sum_k C_{kk,0} - (2\alpha^2)^{-1} \sum_k C_{kk,0}\right) \right. \end{aligned} \quad (165)$$

$$\left. + 2(2\alpha)^{-1} \sum_k C_{kk,0} \frac{1}{2} \sum_k \lambda_k \right] \quad (166)$$

$$= \phi \left[ \left(1 - \frac{\alpha}{2} \sum_k \lambda_k\right) \left(\frac{1}{\nu} - 1\right) + \alpha \sum_k \lambda_k \right] \quad (167)$$

$$= \phi \left[ \left(\frac{1}{\nu} - 1\right) + \alpha \left(\frac{3}{2} - \frac{1}{2\nu}\right) \sum_k \lambda_k \right] \quad (168)$$

implying statement 1:

$$\alpha_{\text{opt}} = \frac{2(\nu-1)}{3\nu-1} \left( \sum_k \lambda_k \right)^{-1}. \quad (169)$$

Next,

$$\partial_\beta L_{\text{approx}}(t)|_{\beta=0} = \phi \left[ (1 - \tilde{U}(1)) [\tilde{V}(1) \partial_\beta (1-\beta)^{-1/\nu} + (1-\beta)^{-1/\nu} \partial_\beta \tilde{V}(1)] \right. \quad (170)$$

$$\left. + 2(1-\beta)^{-1/\nu} \tilde{V}(1) \partial_\beta \tilde{U}(1) \right] \Big|_{\beta=0} \quad (171)$$

$$\begin{aligned} &= \phi \left[ \left(1 - \frac{\alpha}{2} \sum_k \lambda_k\right) \left(\frac{(2\alpha)^{-1}}{\nu(1-\beta)} \sum_k C_{kk,0} - (2\alpha)^{-1} \sum_k C_{kk,0} (1 - \alpha \lambda_k)\right) \right. \\ &\quad \left. + 2(2\alpha)^{-1} \sum_k C_{kk,0} \frac{\alpha}{2} \sum_k \lambda_k (1 - \alpha \lambda_k) \right] \Big|_{\beta=0} \end{aligned} \quad (172)$$

$$= \phi \left[ \left(1 - \frac{\alpha}{2} \sum_k \lambda_k\right) \left(\frac{1}{\nu} - 1\right) \sum_k C_{kk,0} \right. \quad (173)$$

$$\left. + \alpha \sum_k C_{kk,0} \lambda_k \right) + \alpha \sum_k C_{kk,0} \left( \sum_k \lambda_k - \alpha \sum_k \lambda_k^2 \right) \Big]. \quad (174)$$

Substituting  $\alpha = \alpha_{\text{opt}}$ , we find

$$\begin{aligned} \partial_\beta L_{\text{approx}}(t) \Big|_{\substack{\beta=0 \\ \alpha=\alpha_{\text{opt}}}} &= \phi \left[ \frac{2\nu}{3\nu-1} \left( \left(\frac{1}{\nu} - 1\right) \sum_k C_{kk,0} + \left(\sum_k \lambda_k\right)^{-1} \frac{2(\nu-1)}{3\nu-1} \sum_k C_{kk,0} \lambda_k \right) \right. \\ &\quad \left. + \left(\sum_k \lambda_k\right)^{-1} \frac{2(\nu-1)}{3\nu-1} \sum_k C_{kk,0} \left( \sum_k \lambda_k - \left(\sum_k \lambda_k\right)^{-1} \frac{2(\nu-1)}{3\nu-1} \sum_k \lambda_k^2 \right) \right] \\ &= \phi \left[ \nu \sum_k \lambda_k \sum_k C_{kk,0} \lambda_k - (\nu-1) \sum_k C_{kk,0} \sum_k \lambda_k^2 \right], \end{aligned} \quad (175)$$

proving statement 2.  $\square$

In Figure 4 we illustrate this result for a range of models with exact (not asymptotic) power laws (23) at different  $\nu$  and  $\varkappa$ . In this case, in the noise-dominated regime, characteristic (28) is positive for sufficiently large  $\varkappa$  but negative for smaller  $\varkappa$ . In agreement with Proposition 7, we observe experimentally found optimal  $\beta$  to be negative or positive, respectively.

## E Experiments

### E.1 Training regimes

We have considered four regimes of training with the increasing level of approximation for real network dynamics:



1. **Real neural network (NN).**

We used fully-connected neural network with one hidden layer in the NTK parametrization:

$$f(\mathbf{x}, \mathbf{w}) = \frac{1}{\sqrt{N}} \sum_{l=1}^d \mathbf{w}_l^{(2)} \text{ReLU}(\mathbf{w}_l^{(1)} + b_l)$$

Here  $\mathbf{w}_l^{(1,2)}$  are the weight matrices,  $b_l$  are the biases for neuron  $l$ , and  $d$  is the number of units in the hidden layer. We have used  $D = 1000$  in our experiments. For the sake of simplicity, the network outputs a single value for each input, i.e the classification task is treated as regression to the label with the MSE loss. The model is trained via SGD in the standard way: at each step a subset of size  $b$  is sampled without repetition from the training dataset and the weights are updated according to the equation (1).

2. **Linearized regime with sampled batches (*linearized or sampled*).**

Model outputs  $f(\mathbf{x})$  evolve on the dataset of interest according to the equation (45). At each step a batch of size  $b$  is sampled without replacement from the whole dataset of size  $N$  and SGD step is performed.

3. **All second matrix moments dynamics (*all sm*).**

We simulate the dynamics of the whole second moment matrix that is obtained after taking expectation over all possible noise configurations, defined by (56) with the noise term given in the last line of (58).

4. **Spectral diagonal regime (SD).**

In the spectral diagonal regime, the diagonal of the second moment matrix is invariant under SGD dynamics, i.e diagonal elements evolve independently from off-diagonal terms. Therefore, one needs to keep track only of the diagonal terms. The dynamics in the output space follows Eq. (63).

## E.2 Datasets

In the experiments we have used synthetic data with the NTK spectrum and second moment matrix obeying a power-law decay rule  $\lambda_k = k^{-\nu}$  and  $\lambda_k C_{kk,0} = k^{-\varkappa-1}$  with specific  $\nu$  and  $\varkappa$  and the subset of size  $N$  of the MNIST dataset. The whole train dataset of size 60000 requires much memory for the computation of NTK and is too costly from computational side for running large series of experiments, therefore we have used only part of the data of size 1000 – 10000 depending on the experiment. The digits are distributed uniformly in the dataset, i.e there are  $\frac{N}{10}$  samples of each class. We have observed that this subset of data is sufficient to approximate the power-law asymptotic for NTK and partial sums since the exponents do not change significantly with the increase of the amount of data.

## E.3 Experimental details

For Fig. 1 one we have taken a subset of  $N = 3000$  digits from MNIST and ran  $10^4$  SGD updates for the real neural network with one hidden layer, linearized dynamics, and in the spectral diagonal approximation with  $\tau = \pm 1$ . One can see that  $\tau = 1$  provides more accurate approximation for smaller batch size  $b = 10$ , whereas for  $b = 100$  both  $\tau = \pm 1$  are rather accurate.

For Fig. 2 we ran 10000 gradient descent updates for every point on the grid of learning rates  $\alpha$  and  $\beta$ , where we have taken 100 values of  $\alpha$  uniformly selected on  $[0, 4]$  and 50 values for  $\beta$  uniformly on  $[0, 1]$ . The grey regions on the 2d plots correspond to the values of  $\alpha$  and  $\beta$  for which the optimization procedure has diverged. The size of the dataset is 1000 both in the synthetic and MNIST case.

For Figs 5, 4 (left, center and right) we have taken the dataset of size  $N = 10000$  both for synthetic and MNIST case and performed 10000 steps of gradient descent. In Fig. 4 (center) we have taken 100 points uniformly on the interval  $\alpha \in [0, 0.5]$ , and 100 points uniformly on the interval  $\beta \in [-0.3, 0.3]$  for Fig. 4 (right). Concerning the correspondence of optimal learning rates 4 with the analytical formula (158) we observe that is quite accurate for large ratio  $\kappa/\nu$  since the ratio  $\frac{C_{\text{noise}}}{C_{\text{signal}}} \simeq 100$  for  $(\nu, \varkappa) = (1.5, 3.5), (2.0, 5.0)$ , whereas for  $\frac{C_{\text{noise}}}{C_{\text{signal}}} \simeq 1$  for  $(\nu, \varkappa) = (1.5, 2.5), (2.0, 3.5)$ , therefore both the signal and noise asymptotic are of same order for quite a long time, since the difference between the 'signal' exponent  $\xi$  and 'noisy'  $2 - \frac{1}{\nu}$  is relatively small.

#### E.4 Additional experiments

In addition to the experiments with MNIST and synthetic data we ran experiments with real neural networks and with the approximate dynamics for two more datasets from UCI Machine Learning Repository: Bike Sharing dataset <sup>2</sup> and SGEMM GPU kernel performance dataset <sup>3</sup>. The former is a regression problem, namely, prediction of the count of rental bikes per hour or per day, and we've selected the per hour dataset. There are 17389 instances in the dataset and 16 features per input sample. The latter is a regression problem as well, there are 14 features, describing the different properties of the computation hardware and software and the outputs are the execution times of 4 runs of matrix-matrix product for two matrices of size  $2048 \times 2048$ . We predict the average of four runs. There are 241600 instances in the dataset. See results in Figures 6 and 7.

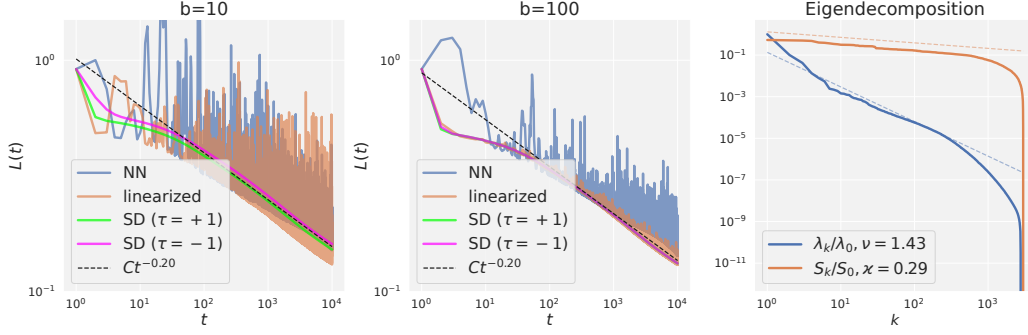


Figure 6: Loss trajectories and spectrum for Bike Sharing dataset. All notations follow Fig. 1. The power-law exponents are  $\nu \simeq 1.43$ ,  $\varkappa \simeq 0.29$ ,  $\zeta \simeq 0.20$

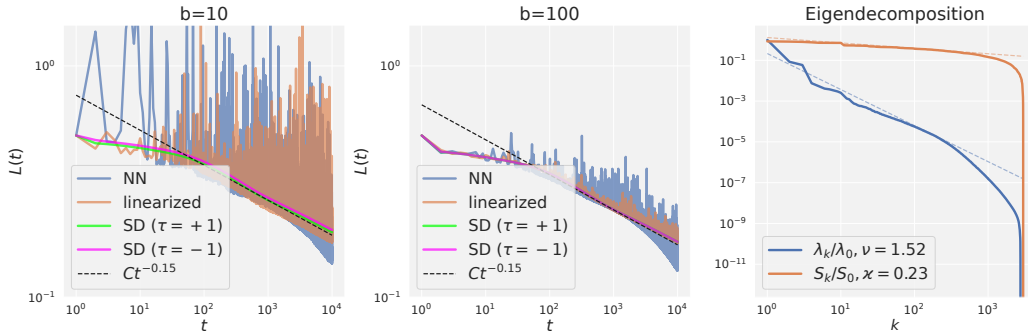


Figure 7: Loss trajectories and spectrum for Sgemm GPU kernel performance dataset. All notations follow Fig. 1. The power-law exponents are  $\nu \simeq 1.52$ ,  $\varkappa \simeq 0.23$ ,  $\zeta \simeq 0.15$

In order to investigate the problem of the loss convergence and determination of the critical learning rate we performed experiments with different batch sizes  $b = 1, 10, 1000, 10000$  on MNIST and synthetic data with  $\nu = 1.5$ ,  $\varkappa = 0.75$  (the 'signal' regime) and with  $\nu = 1.5$ ,  $\varkappa = 3.0$  (the 'noisy' regime). For each value of momentum  $\beta$  we plot the critical value of learning rate  $\alpha_{\text{crit}}$  such that the dynamics starts to diverge. See results in Figures 8, 9 and 10.

#### E.5 Validity of spectral diagonal approximation

In order to check the validity of spectral diagonal approximation and determine the optimal value for parameter  $\tau$  defined in (6) we plotted loss trajectories for linearized dynamics with stochastic sampling of batches, all second moment dynamics, and spectral diagonal approximation with different values of parameter  $\tau$ , see Figure E.5. It turns out that the optimal value of  $\tau$  may vary across different

<sup>2</sup><https://archive.ics.uci.edu/ml/datasets/Bike+Sharing+Dataset>

<sup>3</sup><https://archive.ics.uci.edu/ml/datasets/SGEMM+GPU+kernel+performance>

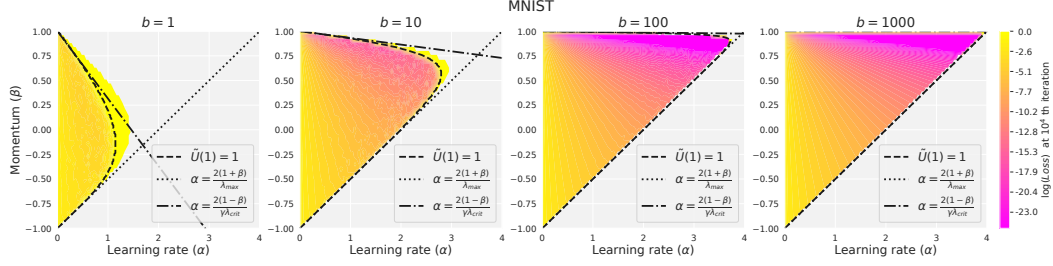


Figure 8:  $L(t = 10^4)$  for different learning rates  $\alpha$ , momenta  $\beta$  and batch sizes  $b$  on MNIST. Legend and notations follow Fig. 2

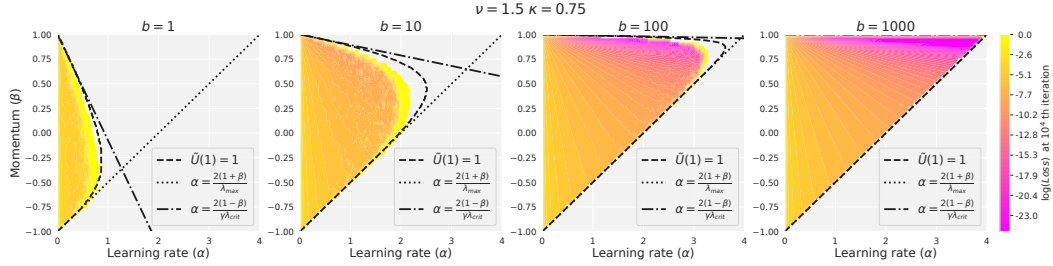


Figure 9:  $L(t = 10^4)$  for different learning rates  $\alpha$ , momenta  $\beta$  and batch sizes  $b$  on synthetic dataset with  $\nu = 1.5$  and  $\kappa = 0.75$ . Legend and notations follow Fig. 2

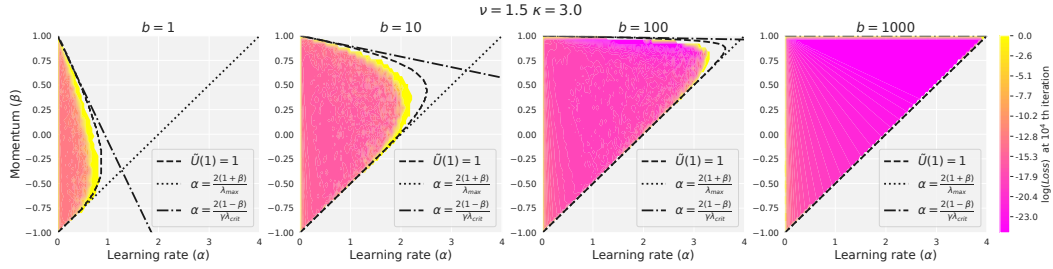


Figure 10:  $L(t = 10^4)$  for different learning rates  $\alpha$ , momenta  $\beta$  and batch sizes  $b$  on synthetic dataset with  $\nu = 1.5$  and  $\kappa = 3.0$ . Legend and notations follow Fig. 2

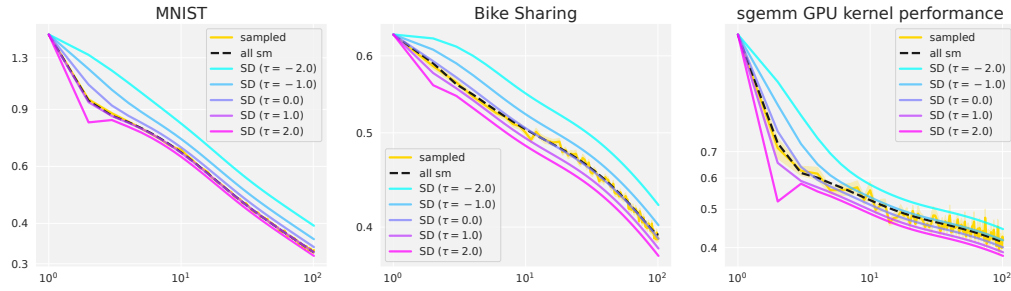


Figure 11: Loss trajectories for linearized stochastic loss dynamics (*solid yellow*), exact simulation of the loss dynamics with full second matrix (*dashed black*) (53), and the loss trajectories for several values of  $\tau$  (shown with different colors). Linearized dynamics with stochastic sampling of batches is averaged over 1000 runs.

datasets. One can observe that for MNIST  $\tau = 1$  seems to be optimal, whereas for the Bike sharing dataset the optimal  $\tau$  is closer to 0, and to  $-1$  for the Sgemm GPU kernel performance dataset.

## F Mini-batch SGD vs. SGD with additive noise

In the paper we considered SGD with the natural noise structure induced by random sampling of batches. However, it is instructive to consider SGD with an additive noise model and observe how this surrogate noise model qualitatively changes optimization. Specifically, we will assume that on each iteration, a Gaussian vector with covariance  $\mathbf{G}$  is added to the true loss gradient:  $\nabla_{\mathbf{w}}^{(t)} L(\mathbf{w}) = \nabla_{\mathbf{w}} L(\mathbf{w}) + \mathbf{g}_t$ ,  $\mathbf{g}_t \sim \mathcal{N}(0, \mathbf{G})$ . For quadratic problems the SGD iteration becomes

$$\begin{pmatrix} \Delta \mathbf{w}_{t+1} \\ \mathbf{v}_{t+1} \end{pmatrix} = \begin{pmatrix} \mathbf{I} - \alpha_t \mathbf{H} & \beta_t \mathbf{I} \\ -\alpha_t \mathbf{H} & \beta_t \mathbf{I} \end{pmatrix} \begin{pmatrix} \Delta \mathbf{w}_t \\ \mathbf{v}_t \end{pmatrix} - \alpha_t \begin{pmatrix} \mathbf{g}_t \\ \mathbf{g}_t \end{pmatrix} \quad (176)$$

Then, due to  $\mathbb{E}[\mathbf{g}_t] = 0$ , the dynamics of first moments is identical to that of noiseless GD, like in the case of sampling noise. However, dynamics of second moments is different:

$$\Sigma_{t+1} = \begin{pmatrix} \mathbf{I} - \alpha_t \mathbf{H} & \beta_t \mathbf{I} \\ -\alpha_t \mathbf{H} & \beta_t \mathbf{I} \end{pmatrix} \Sigma_t \begin{pmatrix} \mathbf{I} - \alpha_t \mathbf{H} & \beta_t \mathbf{I} \\ -\alpha_t \mathbf{H} & \beta_t \mathbf{I} \end{pmatrix}^T + \alpha_t^2 \mathbf{G} \begin{pmatrix} 1 & 1 \\ 1 & 1 \end{pmatrix} \quad (177)$$

Considering again constant learning rates  $\alpha_t = \alpha$ ,  $\beta_t = \beta$ , we see that by making a linear shift of second moments we get the noiseless dynamics:

$$\Sigma_{t+1} - \Sigma^\infty = \begin{pmatrix} \mathbf{I} - \alpha_t \mathbf{H} & \beta_t \mathbf{I} \\ -\alpha_t \mathbf{H} & \beta_t \mathbf{I} \end{pmatrix} (\Sigma_t - \Sigma^\infty) \begin{pmatrix} \mathbf{I} - \alpha_t \mathbf{H} & \beta_t \mathbf{I} \\ -\alpha_t \mathbf{H} & \beta_t \mathbf{I} \end{pmatrix}^T, \quad (178)$$

where  $\Sigma^\infty$  is the “residual uncertainty” determined from the linear equation

$$\Sigma^\infty - \begin{pmatrix} \mathbf{I} - \alpha_t \mathbf{H} & \beta_t \mathbf{I} \\ -\alpha_t \mathbf{H} & \beta_t \mathbf{I} \end{pmatrix} \Sigma^\infty \begin{pmatrix} \mathbf{I} - \alpha_t \mathbf{H} & \beta_t \mathbf{I} \\ -\alpha_t \mathbf{H} & \beta_t \mathbf{I} \end{pmatrix}^T = \alpha^2 \mathbf{G} \begin{pmatrix} 1 & 1 \\ 1 & 1 \end{pmatrix} \quad (179)$$

For simplicity, let’s restrict ourselves to SGD without momentum ( $\beta = 0$ ). Then in the eigenbasis of  $\mathbf{H}$  we have

$$C_{kk,t+1} - C_{kk}^\infty = (1 - \alpha \lambda_k)^2 (C_{kk,t} - C_{kk}^\infty), \quad C_{kk}^\infty = \frac{\alpha}{\lambda_k(2 - \alpha \lambda_k)} G_{kk} \quad (180)$$

Thus, optimization converges with the speed of noiseless GD, but the limiting loss is nonzero:

$$\lim_{t \rightarrow \infty} L(\mathbf{w}_t) = L^\infty = \frac{1}{2} \sum_k \lambda_k C_{kk}^\infty > 0. \quad (181)$$

The key difference of SGD with sampling noise (4), (5) is the multiplicative character of the noise, in the sense that it vanishes as the optimization converges to the true solution and  $\Sigma_t$  becomes close to 0. To summarize, the two largest differences between SGD with additive and multiplicative noises are

1. Loss converges to a value  $L^\infty > 0$  for additive noise and to 0 for multiplicative noise.
2. Convergence rate is independent of noise strength for additive noise, but significantly depends on it for multiplicative noise.

## G Noiseless convergence condition

The convergence condition  $\alpha < \frac{2(1+\beta)}{\lambda_{\max}}$  for noiseless GD is known (see e.g. [45]). For completeness, below we present its derivation in our setting.

First observe that, in the noiseless GD, different eigenspaces of  $\mathbf{H}$  evolve independently from each other. Thus we need to separately require convergence in each eigenspace of  $\mathbf{H}$ . Denoting the eigenvalue of the chosen subspace by  $\lambda$ , we write the GD iteration as

$$\begin{pmatrix} \Delta \mathbf{w}_{t+1} \\ \mathbf{v}_{t+1} \end{pmatrix} = \mathbf{S} \begin{pmatrix} \Delta \mathbf{w}_t \\ \mathbf{v}_t \end{pmatrix}, \quad \mathbf{S} = \begin{pmatrix} 1 - \alpha \lambda & \beta \\ -\alpha \lambda & \beta \end{pmatrix} \quad (182)$$

The characteristic equation for eigenvalues  $s$  of matrix  $\mathbf{S}$  is

$$s^2 - (1 - \alpha \lambda + \beta)s + \beta = 0, \quad (183)$$

yielding solutions

$$s_{1,2} = \frac{1 - \alpha\lambda + \beta \pm \sqrt{(1 - \alpha\lambda + \beta)^2 - 4\beta}}{2} \quad (184)$$

The GD dynamics converges iff  $|s_1| < 1$  and  $|s_2| < 1$ . First note that  $|s_1||s_2| = |\beta|$  and therefore for  $|\beta| \geq 1$  at least one of  $|s_{1,2}|$  will be  $\geq 1$  and GD will not converge. Therefore we only need to consider  $\beta \in (-1, 1)$ .

When  $\beta \in ((1 - \sqrt{\alpha\lambda})^2, (1 + \sqrt{\alpha\lambda})^2)$ , the eigenvalues  $s_{1,2}$  are complex and  $|s_1| = |s_2| = \sqrt{|\beta|}$ . The convergence condition in this region is  $|\beta| < 1$  which is automatically satisfied.

Now consider the region where  $s_{1,2}$  are real. As  $s_1 > s_2$ , the convergence conditions in this region are  $s_1 < 1$  and  $s_2 > -1$ . Note that for  $\beta \leq 0$  the eigenvalues  $s_{1,2}$  are always real, while for  $\beta > 0$  they are real for  $\lambda \in [0, \infty) \setminus (\lambda_1, \lambda_2)$  with  $\lambda_1 = (1 - \sqrt{\beta})^2/\alpha$  and  $\lambda_2 = (1 + \sqrt{\beta})^2/\alpha$ .

Let us first check the condition  $s_1 < 1$ . The equation  $s_1(\lambda) = 1$  gives  $\lambda = 0$ . For  $\beta > 0$  we have  $s_1(\lambda = 0) = 1$ ,  $s_1(\lambda = \lambda_1) = \sqrt{\beta} < 1$  and  $s_1(\lambda = \lambda_2) = -\sqrt{\beta} < 1$  and therefore  $s_1(\lambda) < 1$  on  $(0, \infty) \setminus (\lambda_1, \lambda_2)$  due to continuity of  $s_1(\lambda)$ . For  $\beta < 0$  the condition  $s_1(\lambda) < 1$  is always satisfied because  $s_1(\lambda)$  is decreasing with  $\lambda$ .

Proceeding to condition  $s_2 > -1$  we find that equation  $s_2(\lambda^*) = -1$  gives  $\alpha\lambda^* = 2(\beta + 1)$ . Note that  $\lambda^* > \lambda_2$ . For  $\beta > 0$  we have  $s_2(\lambda = 0) = \beta > -1$ ,  $s_2(\lambda = \lambda_1) = \sqrt{\beta} > -1$ ,  $s_2(\lambda = \lambda_2) = -\sqrt{\beta} > -1$  and  $s_2(\lambda \rightarrow \infty) \rightarrow -\infty$ . Therefore, due to continuity of  $s_2(\lambda)$ , we have  $s_2(\lambda) > -1$  on  $(0, \lambda^*) \setminus (\lambda_1, \lambda_2)$  and  $s_2(\lambda) < -1$  on  $(\lambda^*, \infty)$ . Similarly, for  $\beta < 0$  we again have  $s_2(\lambda) > -1$  on  $(0, \lambda^*)$  and  $s_2(\lambda) < -1$  on  $(\lambda^*, \infty)$ .

Combining all the observations above and we get a single convergence condition for non-stochastic GD:

$$\alpha < \frac{2(1 + \beta)}{\lambda_{\max}}, \quad \beta \in (-1, 1) \quad (185)$$

where  $\lambda_{\max}$  is the largest eigenvalues of  $\mathbf{H}$ .